Extracting Information from the Temperature Gradients of Polypeptide NH Chemical Shifts. 1. The Importance of Conformational Averaging

Niels H. Andersen,* Jonathan W. Neidigh, Scott M. Harris, Gregory M. Lee, Zhihong Liu, and Hui Tong

Contribution from the Chemistry Department, Biophysics Program, University of Washington, Seattle, Washington 98195

Received September 16, 1996. Revised Manuscript Received May 20, 1997[⊗]

Abstract: A detailed analysis of backbone amide NH chemical shift temperature gradients ($\Delta\delta/\Delta T$ values) for proteins and highly cross-linked peptides reveals that hydrogen-bonded exchange-protected NHs are characterized by $\Delta\delta/\Delta T$ values of -2.0 ± 1.4 ppb/°C while exposed NHs typically display gradients of $-6.0 \rightarrow -8.5$ ppb/°C; however, numerous exceptions to these generalizations occur. For partially folded peptides (rather than proteins), exceptions are more common than concordance with this rule; $\Delta\delta/\Delta T$ values ranging from -28 to $+12$ ppb/°C have been observed. In the case of the peptide systems for which exchange protection data is available, the common practice of assuming that a $\Delta\delta/\Delta T$ value less negative than -4 ppb/°C indicates that the NH is sequestered from solvent is shown to have zero predictive validity. The analysis of the data for partially folded peptides, protein fragments, and other peptides which are expected to display minimal structuring reveals a significant correlation between $\Delta\delta/\Delta T$ and the deviation of δ_{NH} from the random coil reference shift. The analysis was facilitated by plotting NH chemical shift deviations (NH-CSD) *versus* the $\Delta\delta/\Delta T$ values. Using such plots, slow-exchanging hydrogen-bonded sites in proteins can be determined with much higher confidence than using the value of the gradient alone. For peptides, the occurrence of large shift deviations *and* abnormal gradients are diagnostic for partial structuring at lower temperatures which becomes increasingly randomized on warming. A good correlation coefficient ($R \geq 0.75$) for NH-CSD and $\Delta\delta/\Delta T$ values indicates that essentially all of the NH shift deviation from reference values is due to the concerted formation of a single structured state on cooling. Correlation coefficients greater than 0.95 were observed for both helix and β-hairpin forming peptides. The slope of the correlation plot (parts per thousand/°C) is a measure of the decrease in the population of the structured state upon warming. A detailed model which rationalizes the effects of conformational equilibria upon NH shifts is presented. A positive ΔCp for unfolding is required to rationalize the linearity of δ_{NH} with temperature that is routinely observed for partially structured peptides. This analysis suggests that ordered states of short peptides achieve significant populations in water only when the hydrophobic effect favors the structured state. This conclusion is pertinent to the current questions concerning the temporal sequence of secondary *versus* tertiary structure formation during protein folding. Further, it is suggested that the use of NMR parameters (scalar and dipolar couplings) to derive the structural preferences of protein fragments which might serve a "seeding" role in the folding pathway is justified only when the CSD/gradient plot displays both a correlation coefficient greater than 0.70 and significant NH-CSD values ($|CSD| > 0.3$).

With the development of 2D NMR methods, peptide/protein structure elucidation has been dominated by methods based on NOE-derived distance constraints. But these methods, which work so well for globular proteins,[1] are now known[2] to be rather ill-suited to peptides that display conformational versatility. Chemical shifts are once again becoming a source of structural insights in studies of peptides and proteins, particularly as chemical shift indices[3] or deviations ($CSD = \delta_{obs} - \delta_{rc}$, where δ_{rc} is a reference "random coil" value). α-Methine CSDs predominantly reflect the ϕ/Ψ values of that specific residue.[4] A periodicity of NH shifts in amphipathic helices has been noted,[5] and a general trend from positive to negative shift deviations along the sequence in proceeding from the N-cap to C-terminus of helices (attributed to the helix macrodipole[3d]) is also commonly observed. Even with the recent publication[6] of two sets of random coil shift values, the authors still urge extreme caution in using NH-CSDs as a source of structural insights. Including anisotropy and electrostatic contributions to amide chemical shifts does not improve the accuracy of structure-based chemical shift predictions;[7] hydrogen bonding

[⊗] Abstract published in *Advance ACS Abstracts,* September 1, 1997.

(1) (a) Clore, G. M.; Gronenborn, A. M. *NMR of Proteins*; CRC Press: Boca Raton, FL, 1993; Chapter 1, pp 1−32. (b) Case, D. A.; Wright, P. E. *NMR of Proteins*; CRC Press: Boca Raton, FL, 1993; Chapter 3, pp 53−91.

(2) (a) Dyson, H. J.; Wright, P. E. *Annu. Rev. Biophys. Chem.* **1991**, *20*, 519−538. (b) Kessler, H.; Griesinger, C.; Müller, A.; Lautz, J.; van Gunsteren, W. F.; Berendsen, H. J. C. *J. Am. Chem. Soc.* **1988**, *110*, 3393−3396. (c) Andersen, N. H.; Chen, C.; Marschner, T. M.; Krystek, S. R., Jr.; Bassolino, D. A. *Biochemistry* **1992**, *31*, 1280−1295. (d) Constantine, K. L.; Mueller, L.; Andersen, N. H.; Tong, H.; Wandler, C. F.; Friedrichs, M. S.; Bruccoleri, R. E. *J. Am. Chem. Soc.* **1995**, *117*, 10841−10854.

(3) (a) Jiménez, M. A.; Nieto, J. L.; Herranz, J.; Rico, M.; Santoro, J. *FEBS Lett.* **1987**, *221*, 320−324. (b) Szilagyi, L.; Jardetzky, O. *J. Magn. Reson.* **1989**, *83*, 441−449. (c) Pastore, A.; Saudek, V. *J. Magn. Reson.* **1990**, *90*, 165−176. (d) Wishart, D. S.; Sykes, B. D.; Richards, F. M. *J. Mol. Biol.* **1991**, *222*, 311−333. (e) Wishart, D. S.; Sykes, B. D.; Richards, F. M. *Biochemistry* **1992**, *31*, 1647−1651. (f) Andersen, N. H.; Cao, B.; Chen, C. *Biochem. Biophys. Res. Commun.* **1992**, *184*, 1008−1014. (g) Wishart, D. S.; Sykes, B. D. *Methods Enzymol.* **1994**, *239*, 363−393.

(4) Ösapay, K.; Case, D. A. *J. Biomol. NMR* **1994**, *4*, 215−230.

(5) (a) Blanco, F. J.; Herranz, J.; González, C.; Jiménez, M. A.; Rico, M.; Santoro, J.; Nieto, J. L. *J. Am. Chem. Soc.* **1992**, *114*, 9676−9677. (b) Zhou, N. E.; Zhu, B.-Y.; Sykes, B. D.; Hodges, R. S. *J. Am. Chem. Soc.* **1992**, *114*, 4320−4326. (c) Zhou, N. E.; Kay, C. M.; Sykes, B. D.; Hodges, R. S. *Biochemistry* **1993**, *32*, 6190−6197.

(6) (a) Merutka G.; Dyson, H. J.; Wright, P. E. *J. Biomol. NMR* **1995**, *5*, 14−24. (b) Wishart D. S.; Bigam, C. G.; Holm, A.; Hodges, R. S.; Sykes, B. D. *J. Biomol. NMR* **1995**, *5*, 67−81.

S0002-7863(96)03250-7 CCC: $14.00

and solvation effects are still not adequately understood. However, the theoretically expected correlation of amide-NH chemical shift with H-bond strength[8] has been confirmed both in the protein chemical shift database[3d] and in specific helical peptides:[9] NHs with strong bonding to a backbone carbonyl are far downfield both in β sheets and in the central portions of curved helices.

In a landmark paper,[10] Llinás and Klein provided a cogent rationale for the solvent-induced changes in NH shifts. This has been designated as the "charge relay" model. Using the nomenclature of Llinás and Klein, both carbonyl "protonation" and H-bond donation produce changes in electron density distribution in the amide group. Increasing H-bonding interactions at either site of the amide unit results in larger positive charges at both the ^{15}N and ^{1}H nuclei of the "bonded" amide unit and thus increased chemical shifts. However, in cyclic peptides, and in peptides with partially populated turn conformations, there are instances where presumably H-bonded NHs appear upfield.[10−12]

Amide-NH temperature gradients ($\Delta\delta_{NH}/\Delta T$) have had, in our opinion, a checkered career as a tool for structure investigation in peptides and proteins. The magnitude of $\Delta\delta_{NH}/\Delta T$ has been used to confirm solvent inaccessibility, locate reversing turns,[12c,13] ascertain the changes in the relative populations of such turns in cyclic peptides[10,11,12a] with media changes, and measure changes in turn populations of linear peptides upon residue sustitution.[12b−d,13,14] The seminal accounts[11] noting the effect of amide NH sequestration upon NH $\Delta\delta/\Delta T$ were empirical studies. For several series of cyclic peptides, it was noted that some NHs displayed negative gradients (upfield shifts on warming) similar to an exposed "amide" model, while others, which had either an intramolecular H-bond or were internally directed in the structural model of the peptide, displayed much less negative gradients. Llinás and Klein[10] extended this observation to a wide range of solvents—CF_3CO_2H, CF_3CH_2-OH(TFE), $CHCl_3$, water, DMSO, DMF, and pyridine—stating "the temperature coefficient ... affords an excellent criterion to determine the extent of exposure of the NH group, whatever the solvent." Using the amide solvation model for rationalizing NH temperature gradients, the more rapid upfield shift of solvent-exposed NHs upon warming can be attributed to the relatively larger decrease in intermolecular versus intramolecular H-bonding due to the entropy change associated with intermolecular interactions. It is well-established that random coil peptides display $\Delta\delta_{NH}/\Delta T$ values of -7.8 ± 1.2 ppb/°C in aqueous medium.[6a] Over the years, it has become common practice[15,16] to assume that NHs with gradient values less negative than −4 ppb/°C are sequestered from solvent contact. Many authors who have used this criterion have failed to recognize an implicit assumption, that the conformation of the polypeptide is not changing with temperature.[17] Protection from H/D exchange with the medium should provide a more secure measure of solvent access. However, it has even been suggested that NH $\Delta\delta/\Delta T$ values are most useful when the H-bonding interaction is not stable enough for measurable solvent exchange protection,[18] a common observation in partially structured peptides. It is in peptides, where increased temperature generally favors the random coil state, that $\Delta\delta_{NH}/\Delta T$ values are most often employed as a structural determinant. Since $\Delta\delta_{NH}/\Delta T$ values are much more readily measured than exchange protection factors, we suspect that many errors have resulted when it was assumed that small gradients reflect NH sequestration in a dominant structured form.

It is possible to predict, *a priori*, the temperature dependence of NH chemical shifts for two cases: a rigid structure and a temperature-dependent structured state to random coil transition. First, for a rigidly structured state, an intramolecular H-bonded NH should be downfield and have a very small negative $\Delta\delta_{NH}/\Delta T$ while the solvent-exposed NHs should have shifts and temperature gradients that are affected primarily by H-bonding to solvent and will be more similar to random coil values.

For the second case, the observed chemical shifts will be population-weighted averages of the shifts in the structured and random coil states at each temperature. As the temperature is increased and the random coil state becomes more populated, the observed shifts will move toward their random coil values. Thus the observed temperature dependence of the amide chemical shift will reflect both the intrinsic temperature gradient of each state *and* the temperature-dependent equilibrium between the structured and random coil states. A correlation between chemical shift (specifically the deviation from the random coil value caused by structuring) and the temperature gradient is thus expected. This correlation should reflect the influence of temperature on the structured state → random coil transition equilibrium. We first noted this type of correlation between NH CSD- and $\Delta\delta/\Delta T$ values for those portions of an endothelin sequence which existed as a mixture of conformers that becomes more nearly random as the temperature is increased.[2c] Small negative and even positive temperature gradients were found for rapidly exchanging NHs which displayed an upfield shift in the dominant conformer; slow exchanging NHs that were far downfield displayed temperature gradients similar to, or more negative than, those expected for exposed NHs. Subsequent studies[19] of peptides have confirmed that, upon warming, downfield NH resonances tend to shift upfield more rapidly than NHs with an upfield shift nearly independent of their degree of solvent exchange protection. The implicit caution concerning the use of $\Delta\delta/\Delta T$ values to judge NH solvent accessibility has

(7) Ösapay, K.; Case, D. A. *J. Am. Chem. Soc.* **1991**, *113*, 9436−9444.
(8) Popov, E. M.; Zheltova, V. N. *J. Mol. Struct.* **1971**, *10*, 221−230.
(9) Andersen, N. H.; Cort, J. R.; Harris, S. M.; Lee, G. M.; Liu, Z.; Neidigh, J. W.; Tomaszewski, J. W.; Tong, T. Presented at the 36th Experimental NMR Conference, Boston, MA, March 1995, Abstract P-134, p 165.
(10) Llinás, M.; Klein, M. P. *J. Am. Chem. Soc.* **1975**, *97*, 4731−4737.
(11) (a) Kopple K. D.; Ohnishi, M.; and Go. A. *J. Am. Chem. Soc.* **1969**, *91*, 4264−4274. (b) Ohnishi, M.; Urry, D. W. *Biochem. Biophys. Res. Commun.* **1969**, 36, 194−202.
(12) (a) Krystek, S. R., Jr.; Bassolino, D. A.; Bruccoleri, R. E.; Hunt, J. T.; Porubcan, M. A.; Wandler, C. F.; Andersen, N. H. *FEBS Lett.* **1992**, *299*, 255−261. (b) Dyson, H. J.; Satterthwait, A. C.; Lerner, R. A.; Wright, P. E. *Biochemistry* **1990**, *29*, 7828−7837. (c) Bisang, C.; Weber, C.; Inglis, J.; Schiffer, C. A.; vanGunsteren, W. F.; Jelesarov, L.; Bosshard, H. R.; Robinson, J. A. *J. Am. Chem. Soc.* **1995**, *117*, 7904−7915. (d) Campbell, A. P.; Sykes, B. D.; Norrby, E.; Assa-Munt, N.; Dyson, H. J. *Folding Des.* **1996**, *1*, 157−165.
(13) (a) Andersen, N. H.; Hammen, P. K. *Biorg. Med. Chem. Lett.* **1991**, *1*, 263−266. (b) Dyson, H. J.; Rance, R.; Houghten, R. A.; Lerner, R. A.; Wright, P. E. *J Mol. Biol.* **1988**, *201*, 161−200.
(14) Wright, P. E.; Dyson, H. J.; Lerner, R. A. *Biochemistry* **1988**, *27*, 7167−7175.
(15) Jiménez, M. A.; Nieto, J. L., Rico, M.; Santoro, J., Herranz, J.; Bermejo, F. J. *J. Mol. Struct.* **1986**, *143*, 435−438.
(16) Zimmermann G. R.; Legault, P.; Selsted, M. E.; Pardi, A. *Biochemistry* **1995**, *34*, 13663−13671.
(17) In at least 19 of the publications cited in this paper, the authors have employed reduced NH shift temperature gradients as basis for assigning or confirming NH sequestration; nine of these reports appearing after our warning[2c] that conformer population changes can result in even larger effects than changes in solvent interactions. In one endothelin paper (Reily, M. D.; Dunbar, J. B., Jr. *Biochem. Biophys. Res. Commun.* **1991**, *178*, 570−577), the low gradients displayed by NHs at residues 8−11 even persuaded the authors that it is the N-terminal turn of an α helix that has hydrogen-bonded NHs.
(18) Williamson, M. P.; Waltho, J. P. *Chem. Soc. Rev.* **1992**, 227−236.
(19) Posters presented at the annual Experimental NMR Conference—35th ENC, Asilomar, CA, April 1994, Abstract MP-46, p 109; 37th ENC, Asilomar, CA, March 1996, Abstract WP-56, p 250.

been largely ignored.[17] Herein we present (a) an update on this "correlation" for a more extensive $\Delta\delta/\Delta T$-exchange-CSD database for endothelin-related species, (b) a review of $\Delta\delta/\Delta T$ data for proteins where NH exchange protection factors are known, (c) studies of changes in NH chemical shifts and temperature gradients associated with peptide structuring transitions, (d) a novel graphic format for displaying $\Delta\delta/\Delta T$ correlations that yields structural and dynamic insights, and (e) a model of peptide conformational equilibria that rationalizes the linearity of δ_{NH} versus temperature plots and provides a basis for the quantitative interpretation of NH CSD-$\Delta\delta/\Delta T$ correlation plots.

Materials and Methods

Peptides. The salmon calcitonin fragment, VLGKLSQELHKLQ-TYPRTNTGSGTP-NH_2 (sCTf), and pramlintide, the [Pro[25,28,29]] analogue of human pancreatic amylin,[20] were obtained from Kathryn Prickett (Amylin Pharmaceuticals Inc., San Diego, CA). C-peptide analogues RN-44 and RN-103 were gifts from Professor Robert Baldwin (Stanford University). An additional C-peptide analogue (RNACP-1), Ac-AETAK$^{(\epsilon Ac)}$AKFQRAHA-NH_2 [$(M + H)^+$ 1511.9, by fast atom bombardment mass spectrometry], was prepared at the Bristol-Myers Squibb Institute for Pharmaceutical Research by automated solid phase synthesis (Biosearch 9600 peptide synthesizer) using commercial Boc-amino acids (Bachem, Torrance, CA) and the manufacturer recommended protocols. The 2D NMR data reported in the Ph.D. thesis of S. Harris[21] confirm the sequence and that the peptide is increasingly helical as hexafluoro-2-propanol (HFIP) is added. The [Pen[3,11],Nle[7]]-endothelin-1 sample was that employed in previous studies.[22]

CD Sample Preparation and Spectroscopy. Samples were prepared by dissolving weighed amounts (2−4 mg) of freshly vacuum-dried peptides directly in 2 mM aqueous phosphate or acetate buffer (pH 7.5 or 4.0) to produce stock solutions with nominal concentrations of *ca.* 600 μg/mL. The concentrations of the stock solutions were determined by UV for the salmon calcitonin fragment which contains a Tyr chromophore: $\epsilon_{274} - \epsilon_{310} = 1405$ at pH ≤ 7.[23] The concentration of the stock solution of RNACP-1 was based on direct CD comparisons (data not shown) with RN-103 and RN-44 under conditions previously used by the Baldwin group.[24] CD spectra were recorded using a JASCO model J720 spectropolarimeter, which had stabilized for at least 30 min with a nitrogen flow rate of 5 L/min as previously described.[22b,25] CD spectral values for peptides are expressed in units of residue molar ellipticity ((deg·cm^2)/(residue·dmol)). Final peptide concentrations of 20−110 μM in the CD cells (typically of 2−0.5 mm path length) were obtained by quantitative serial dilution of the stock solutions to the required levels of fluoroalcohol and aqueous buffer (10−20 mM acetate and/or phosphate).

NMR Spectroscopy. NMR spectra at 500 MHz were recorded for 2.5−5 mM protein/peptide solutions as previously described;[2c,25a] all temperature gradients were measured by differences observed in spectra recorded at 5−10 °C intervals over at least a 20 °C range. Temperature gradients are expressed in units of ppb/°C with a negative sign indicating an upfield shift upon warming. The salmon calcitonin fragment (sCTf, residues 8−32) was examined throughout the range 275−305 K in aqueous buffer (10 mM acetate, pH 3.66) and in 3:1 aqueous buffer/HFIP. For the C-peptide analogue, the fluoroalcohol titration was performed in the NMR tube; RNACP-1 was dissolved in 3:1 aqueous phosphate buffer (pH 3.4)/methanol with HFIP added to afford 4, 10, and 21 vol % final compositions. At each fluoroalcohol concentration, 2D spectra sufficient for complete assignment were recorded at two or three temperatures over at least a 40° range before additional fluoroalcohol was added. The temperature dependences of the NH shifts of pramlintide were determined from a series of five ^{15}N-HMQC spectra (268−315 K) recorded for the universally ^{15}N-labeled form of pramlintide free acid (prepared by Susan Janes, Amylin Pharmaceuticals) in aqueous HFIP (35 vol % HFIP) with added HCO_2H and CD_3CO_2H to produce a pH of 3.6.

Random Coil Reference Values and Chemical Shift Deviations. Over the last 4 years, we have compiled[21,22c] a set of random coil values from our own and literature peptide and protein data. With the recent availability of three additional sets of "random coil" values,[26a] we have chosen to use the averages of the four sets as "coil" reference values. The resulting values for αH are, with the exceptions of Asp^-, Glu^-, and His^+, 0.02 ± 0.03 ppm downfield of our previous values.[22c] We attribute the 0.23 ppm difference in NH reference values in the two recent publications[6] largely to the "three-effect"[26b] shown below—the nature of the N-terminus was taken into account in averaging the reported values. The resulting mean reference values are given here[27] using the one-letter code for residues, X (NH, αH): A (8.21, 4.32), C (8.23, 4.57), C_2 (8.34, 4.69), D^- (8.29, 4.65), D° or N (8.40, 4.72), E^- (8.37, 4.32), E° or Q (8.27, 4.34), F (8.25, 4.61), G (8.28, 3.96), H^+ (8.35, 4.70), I (8.08, 4.15), K (8.19, 4.32), L (8.17, 4.32), M (8.25, 4.48), Nle (8.22, 4.32), P (−, 4.43), Pen (*8.26*, *4.65*), R (8.24, 4.34), S (8.26, 4.47), T (8.15, 4.37), V (8.08, 4.10), W (8.05, 4.65), and Y (8.13, 4.56 ppm). We have also included working values for two commonly used unnatural residues, norleucine and penicillamine. The values are for 25 °C and a correction of −7.6 ppb/°C (the average "coil state" NH temperature gradient reported by Merutka et al.[6a]) is applied to the NH reference values prior to determining the CSD from experimental data at other temperatures. There is increasing evidence that coil values need to be corrected for sequence postition and nearest neighbor effects.[26b] These corrections are shown below. The effect of a following Pro residue on the αH shift, a 0.29 ppm downfield shift (0.17 for Gly-Xaa), is taken from Wishart et al.[6b]

$$^{+}H_3N\text{-}Xaa^{1}\text{-}NH\text{-}Xaa^{2}\text{-}NH\text{-}Xaa^{3}\ .\ .\ NH\text{-}Xaa\text{-}Pro\ .\ .\ NH\text{-}Xaa^{c-1}\text{-}NH\text{-}Xaa^{c}\text{-}CO_2^-$$
$$-0.26\ \ +0.48\ \ -\ \ +0.2 \qquad +0.29 \qquad -0.43\ \ -0.17$$

The corrections are in all cases applied to the reference values. We have not derived the end effects for a non-protonated N-terminus; when the termini are capped, or in the case of the C-terminus, protonated, the corrections given above are not applied. Our studies also suggest that medium effect corrections are required for both NH shifts and αH shifts. The only corrections employed in the present work are downfield shifts for αH random coil reference values as the fluoroalcohol concentration in the medium is increased—+0.015 (4 vol % HIFP), +0.04 (10 vol % HFIP or 25 vol % TFE), +0.05 (12−16 vol % HFIP, 35−45 vol % HFIP), + 0.075 ppm (25−35 vol % HFIP)—these are somewhat larger than the TFE-induced shifts determined by Merutka *et al.*[6a] The CSD values are calculated as $\delta_{obs} - \delta_{ref}$(corrected); upfield shifts are thus recorded as negative CSD values.

NH CSD-$\Delta\delta/\Delta T$ Correlation Plots. We have found that plots of CSD *versus* $\Delta\delta/\Delta T$ for amide NHs provide significant insights and are a useful tool in polypeptide structure elucidation. The plot is formatted so as to place downfield NH resonances to the left as in typical NMR spectra. The chemical shift deviations are derived from the lowest temperature included in the experiment. The temperature gradient axis is oriented so that amides which display larger upfield shifts on warming are placed toward the top of the graph. Figure 1 provides an example with the axes labeled. Points appearing toward the lower left thus represent NHs that are downfield and which do not

(20) Cort, J.; Liu, Z.; Lee, G.; Harris, S. M.; Prickett, K. S.; Gaeta, L. S. L.; Andersen, N. H. *Biochem. Biophys. Res. Commun.* **1994**, *204*, 1088−1095.

(21) Harris, S. M. Ph.D. Thesis, University of Washington, 1993.

(22) (a) Lee, G. M.; Chen, C.; Marschner, T. M.; Andersen, N. H. *FEBS Lett.* **1994**, *355*, 140−146. (b) Andersen, N. H.; Harris, S. M.; Lee, V. G.; Liu, E. C.-K.; Moreland, S.; Hunt, J. T. *BioOrg. Med. Chem.* **1995**, *3*, 113−124. (c) Andersen, N. H.; Chen, C.; Lee, G. M. *Protein Pept. Lett.* **1995**, *1*, 215−222.

(23) Mihalyi, E. *J. Chem. Eng. Data* **1968**, *13*, 179−182.

(24) (a) RN-44 -- Fairman, R.; Shoemaker, K. R.; York, E. J.; Stewart, J. M.; Baldwin, R. L. *Proteins: Struct., Funct., Genet.* **1989**, *5*, 1−7. (b) RN-103: Shoemaker, K. R.; Fairman, R.; Schultz, D. A.; Robertson, A. D.; York, E. J.; Stewart, J. M.; Baldwin, R. L. *Biopolymers* **1990**, *29*, 1−11.

(25) (a) Andersen, N. H.; Cao, B.; Rodríguez-Romero, A; Arreguin, B. *Biochemistry* **1993**, *32*, 1407−1422. (b) Andersen, N. H.; Palmer, R. B. *BioOrg. Med. Chem. Lett.* **1994**, *4*, 817−822.

(26) (a) One set was a personal communication (January 1995) from Rico and Nieto (CSIC, Madrid), the others have been published.[6] (b) We first noted the two-effect in 1991[2c,12a] and provided corrections for the two- and three-effect in 1995.[22c] These Coulombic effects have also been calculated: Gmeiner, W. H.; Facelli, J. C. *Biopolymers* **1996**, *38*, 573−581.

(27) These values have been published previously: Andersen, N. H.; Liu, Z.; Prickett, K. S. *FEBS Lett.* **1996**, *399*, 47−52.

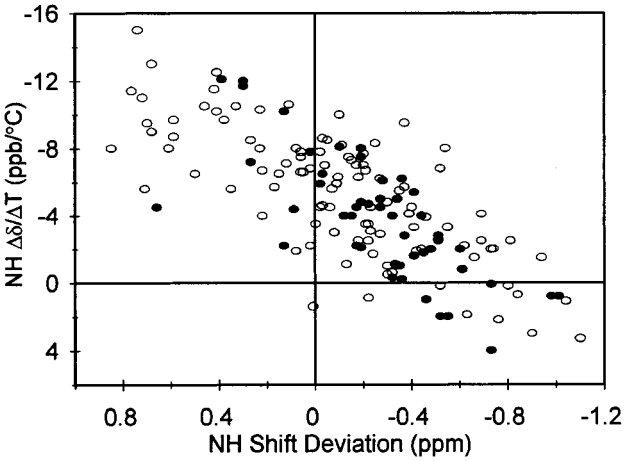

Figure 1. Correlation between NH temperature gradient ($\Delta\delta/\Delta T$ in ppb/°C) and the NH shift deviation from the random coil expectation value (NH-CSD in ppm) observed for endothelin and apamin analogues. Filled symbols correspond to NHs that are significantly protected from solvent exchange. The slow exchanging NHs display a significant correlation coefficient ($R = 0.74$) with a slope of −8.2 ppt/°C for the resulting least-squares line. The open symbols are fast exchanging NHs (slope −6.5; $R = 0.75$).

shift rapidly upfield upon warming; as it turns out, these are very likely to be intramolecularly hydrogen-bonded sites.

Assembly of a Protein/Peptide NH Database. Amide temperature gradient data has been reported (or can be approximated from shift data at two temperatures) for seven proteins (and/or highly cross-linked peptides)—BPTI,[28] ω-Conotoxin GVIA,[29a] Cellobiohydrolase,[29b] Leu^5-EETI-2,[29c] Eglin-c,[30] Interleukin-8,[31] and bNβD12.[16] Hevein,[25a,32] a 43-residue tetradisulfide protein studied in this laboratory, was included with the seven literature proteins to produce our protein NH database (361 data points). Literature reports[33] of the NH shifts and gradients for short-to-medium-length peptide fragments corresponding to the complete sequences of four proteins were used to generate a 399-point database; these fragments are presumably in a random coil state in aqueous medium. Other protein sequence fragments[34,35] are included in Tables 2 and 4. Several of the longer protein fragments have, however, been shown to increasingly adopt a structured state in aqueous TFE.[33e,34c,e,f] Designed peptides that undergo a structure to random coil transition on warming are taken from studies performed in this laboratory and key literature reports.[36−39] The NH NMR database that resulted contains entries for a total of more than 1500 NHs. These entries are listed by both polypeptide structure and by NH category (exchange protected versus rapidly exchanging, H-bonded versus not H-bonded, etc.) in Tables 1, 2, and 4.

For data taken from the literature, the published classification of NHs as slow and fast exchanging was used unless otherwise specified. For hevein, the protection factors were available from studies in this laboratory. In the case of BPTI, the complete set of exchange rates[28c] allowed us to further differentiate NHs as modestly or significantly exchange protected. The publications were also examined for evidence of H-bonding state definition. We have, however, attempted to ignore all H-bonding conclusions in the original paper that were based exclusively on NH $\Delta\delta/\Delta T$ data. NMR structure ensembles, when available from the PDB, were used to ascertain the hydrogen-bonding status. In the case of BPTI, both X-ray[28d] and NMR[28e] structures have been published; the latter (PDB file 1PIT) was employed for the NH H-bonding states classification. An NH is classified as H-bonded when a supermajority (≥60%) of the structures in the ensemble have the same electron pair donor within H-bonding distance (≤2.5 Å) and at angles greater than 120°.

Our published NMR structure[25a] of hevein, which is quite different than the X-ray structure,[40] was recently confirmed by an independent NMR study.[41] A pair of higher precision structures that resulted after a more extensive analysis of the NOESY spectra, which also provided 29 prochiral α/β methylene and 2 Leu-δ,δ' prochirality assignments,[32] now replace the hevein structures in the Protein Data Bank (code 1HEV), and these were used for the present analysis. Two structures were included to present alternative conformers evident in the NMR data. The conformational differences occur at a linked turn locus (Cys^{12}-Pro^{13}-Asn^{14}-Asn^{15}-Leu^{16}), with major (βII/III′) and minor (βI/−) turn states. Essentially complete NH exchange rate and temperature gradient profiles are available for two ionization states (pH 2.4 and 6.6).

Results and Discussion

A reconsideration of endothelin-related peptides, the system in which we first noted a correlation between NH temperature gradients and chemical shift deviations, is presented first to show that NH gradients have no relation to exchange protection in systems that display conformational averaging. This is followed by a consideration of proteins (and the fragments derived therefrom) to examine the usefulness of $\Delta\delta_{NH}/\Delta T$ values where the rigid scaffold assumption of the solvation model is most

(28) (a) Wagner, G.; Wüthrich, K. *J. Mol. Biol.* **1982**, *155*, 347−366. (b) Wagner, G.; Braun, W.; Havel, T. F.; Schaumann, T.; Gô, N.; Wüthrich, K. *J. Mol. Biol.* **1987**, *196*, 611−639. (c) Wagner, G.; Wüthrich, K. *J. Mol. Biol.* **1982**, *160*, 343−361; **1979**, *130*, 1−18. (d) Wlodawer, A.; Deisenhofer, J.; Huber, H. *J. Mol. Biol.* **1987**, *193*, 145−156. (e) Berndt, K. D.; Güntert, P.; Orbons, P. M.; Wüthrich, K. *J. Mol. Biol.* **1992**, *227*, 757−775.

(29) (a) ω-Conotoxin GVIA: Davis J. H.; Bradley, E. K.; Miljanich, G. P.; Nadasdi, L.; Ramachandran, J.; Basus, V. J. *Biochemistry* **1993**, *32*, 7396−7405. (b) Cellobiohydrolase I: Kraulis P. J.; Clore, G. M.; Nilges, M. Jones, T. A.; Pettersson, G.; Knowles, J.; Gronenborn, A. M. *Biochemistry* **1989**, *28*, 7241−7257. (c) [Leu^5]EETI-II: Nielsen, K. J.; Alewood, D.; Andrews, J.; Kent, S. B. H.; Craik, D. J. *Protein Sci.* **1994**, *3*, 291−302.

(30) (a) Hyberts, S. G.; Wagner, G. *Biochemistry* **1990**, *29*, 1465−1474. (b) Hyberts, S. G.; Goldberg, M. S.; Havel T. F.; Wagner, G. *Protein Sci.* **1992**, *1*, 736−751. (c) Heinz D. W.; Hyberts, S. G.; Peng, J. W.; Priestle, J. P.; Wagner, G.; Grütter, M. G. *Biochemistry* **1992**, *31*, 8755−8766.

(31) IL-8: (a) for the $\Delta\delta/\Delta T$ values: Rajarathnam, K.; Clark-Lewis, I.; Sykes, B. D. *Biochemistry* **1994**, *33*, 6623−6630. (b) For the structure derivation, see: Clore, G. M.; Appella, E.; Yamada, M.; Matsushima, K.; Gronenborn, A. M. *J. Biol. Chem.* **1989**, *264*, 18907−18911. (c) Clore G. M.; Appella, E.; Yamada, M.; Matsushima, K.; Gronenborn, A. M. *Biochemistry* **1990**, *29*, 1689−1696.

(32) Cao, B. Ph.D. Thesis, University of Washington, 1993.

(33) (a) Myohemerythrin: Dyson, H. J.; Merutka, G.; Waltho, J. P.; Lerner, R. A.; Wright, P. E. *J. Mol. Biol.* **1992**, *226*, 795−817. (b) Plastocyanin: Dyson, H. J.; Sayre, J. R.; Merutka, G.; Shin, H.; Lerner, R. A.; Wright, P. E. *J. Mol. Biol.* **1992**, *226*, 819−835. (c) BPTI: Kemmink, J.; Creighton, T. E. *J. Mol. Biol.* **1993**, *234*, 861−878. (d) Protein G B1-(2−19): Blanco, F. J.; Jiménez, M. A.; Pineda, A.; Rico, M.; Santoro, J.; Nieto, J. L. *Biochemistry* **1994**, *33*, 6004−6014. (e) Other protein G B1 domain fragments: Blanco, F. J.; Serrano, L. *Eur. J. Chem.* **1995**, *230*, 634−649.

(34) (a) Wang, G.; Pierens, G. K.; Treleaven, W. D.; Sparrow, J. T.; Cushley, R. J. *Biochemistry* **1996**, *35*, 10358−10366. (b) Mendz, G. L.; Barden, J. A.; Martenson, R. *E. Eur. J. Biochem.* **1995**, *231*, 659−666. (c) Odaert, B.; Baleux, F.; Huynh-Dinh, T.; Neumann, J.; Sanson, A. *Biochemistry* **1995**, *34*, 12820−12829. (d) Waltho, J. P., Feher, V. A.; Merutka, G.; Dyson, H. J. Wright, P. E. *Biochemistry* **1993**, *32*, 6337−6347. (e) Maciejewski, M. W.; Zehfus, M. H. *Biochemistry* **1995**, *34*, 5795−5800. (f) Itzhaki, L. S.; Neira, J. L.; Ruiz-Sanz, J.; de Prat, G. G.; Fersth, A. R. *J. Mol. Biol.* **1995**, *254*, 289−304.

(35) (a) Blanco, F. J.; Jiménez, M. A.; Rico, M.; Santoro, J.; Herranz, J.; Nieto, J. L. *Eur. J. Biochem.* **1991**, *200*, 345−351. (b) Neira, J. L.; Fersht, A. R. *Folding Des.* **1996**, *1*, 231−241.

(36) (a) Blanco, F. J.; Jiménez, M. A.; Herranz, J.; Rico, M.; Santoro, J.; Nieto, J. L. *J. Am. Chem. Soc.* **1993**, *115*, 5887−5888. (b) deAlba, E.; Jimenez, M. A.; Rico, M.; Nieto, J. L. *Folding Des.* **1996**, *1*, 133−144. (c) deAlba, E.; Jimenez, M. A.; Rico, M. *J. Am. Chem. Soc.* **1997**, *119*, 175−183.

(37) (a) Bradley E. K.; Thomason, J. F.; Cohen, F. E.; Kosen, P. A.; Kuntz, I. D. *J. Mol. Biol.* **1990**, *215*, 607−622. (b) Merutka G.; Morikis, D.; Bruschweiler, R.; Wright, P. E. *Biochemistry* **1993**, *32*, 13089−13097.

(38) Vinogradov, A. A.; Mari, F.; Humphreys, R. E.; Wright, G. E. *Int. J. Pept. Res.* **1996**, *47*, 467−476.

(39) Rothemund, S.; Weisshoff, H.; Beyermann, M.; Krause, E.; Biernert, M.; Mügge, C.; Sykes, B. D.; Sönnichsen, F. D. *J. Biomol. NMR* **1996**, *8*, 93−97.

(40) Rodríguez-Romero, A; Ravichandran, K. G.; Soriano-García, M. *FEBS Lett.* **1991**, *291*, 307−309.

(41) Asenio, J. L.; Cañada, F. J.; Rodríguez-Romero, A.; Jiménez-Barbero, J. *Eur. J. Biochem.* **1995**, *230*, 621−633.

nearly and least valid. Specific studies of peptides that undergo well-defined structuring transitions and a model for the observed correlation between NH CSD and $\Delta\delta/\Delta T$ is then presented to provide a better understanding of the gradients when a temperature-dependent structuring transition is present.

Endothelin and Apamin Analogues. The observed NH shift temperature gradients for endothelin-1 in aqueous glycol[2c] sparked this investigation. We have now completed NMR structure elucidations for several additional endothelin analogues,[22,42] including ones in which each of the disulfides were absent (C → A) or altered (C → Pen) and in which an endothelin-like sequence was present but the disulfide linkages were those of apamin.[43] Other groups have reported both NH exchange data and temperature gradients for endothelin mutants (including other monocyclic species)[44] and for monocyclic analogues[45] of apamin. With both sequences and linkage pattern included, this is a diverse collection of peptides. This is evidenced by the lack of consistency in the identity of the residues displaying the extreme upfield or downfield shifted NH resonances. These are indicated by arrows (→, upfield; ←, downfield) on the native sequences.

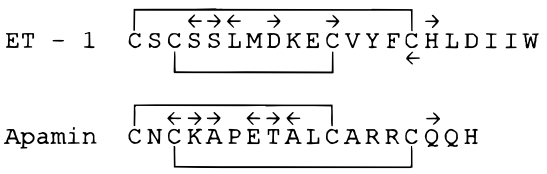

When the disulfide deletion analogues and point mutants are included, the identities of the residues in each category (downfield/upfield shifted, etc.) is even more diverse. The correlation between shift deviation, protection, and $\Delta\delta/\Delta T$ values for the resulting 153 point data set is shown in Figure 1. Exchange-protected (10× or greater protection factors) NHs are shown as filled symbols.

Even a cursory examination of Figure 1 shows that any attempt to divine whether amide NHs are solvent protected or exposed using the gradients would be extremely misleading. This figure employs a plot format (see the Materials and Methods) for experimental NH $\Delta\delta/\Delta T$ and CSD values which we have found to be particularly revealing. In this data set, slow exchanging NHs display $\Delta\delta/\Delta T$ values from −12.1 to +4.0, $-3.78 \pm 3.6°$ ($n = 49$), barely different than the statistics for the fast exchanging groups, range −15 to +3.3, -5.35 ± 3.8^2 ($n = 104$). Instead of a correlation between NH $\Delta\delta/\Delta T$ and exchange protection, a reliable indicator of intramolecular hydrogen-bond formation, the gradients correlate ($R = 0.75$) with shift deviation irrespective of exchange protection, see Table 1. This larger data set for endothelin/apamin analogues confirms our earlier conclusion[2c] that $\Delta\delta/\Delta T$ values become more negative as NHs are shifted downfield relative to their "coil" shift values due to "structuring".

These peptides display a much larger range of NH temperature gradients than would be expected on the basis of the currently accepted solvent exposure model. If the NH temperature gradients result from the interaction of a temperature-invariant structure with the solvent, all the gradients should be between −9 and 0 ppb/°C. The endothelin and apamin analogues have a significant number of $\Delta\delta_{NH}/\Delta T$ values outside this range. We suggest that the abnormal gradients displayed by these and other peptides signal the presence of a temperature-dependent structure/disorder transition.

Table 1. Least-Squares Correlations of NH Shift Deviations and Temperature Gradients for Endothelin and Apamin Analogues

			least-squares ($\Delta\delta/\Delta T$, CSD) correlation[a]			
	$\langle\Delta\delta/\Delta T\rangle$ (se)	n	$\Delta\delta/\Delta T$, CSD = 0	S_{res}[a]	slope	R
all	−4.86 (3.81)	153	−5.91 (0.22)	2.53	−6.92	0.75
slow exchanging	−3.78 (3.60)	49	−5.94 (0.45)	2.46	−8.17	0.74
fast exchanging	−5.35 (3.82)	104	−6.01 (0.26)	2.55	−6.47	0.75
loci of change	−5.81 (4.18)	20	−6.40 (0.49)	2.17	−7.15	0.87
other fast	−5.26 (3.70)	84	−5.90 (0.30)	2.64	−6.23	0.71

[a] The first column in the least-squares correlation area is the values of $\Delta\delta/\Delta T$ at the intercept (that is at CSD = 0) and its standard error (se). The second column is the error of estimation (S_{res}) for $\Delta\delta/\Delta T$ based on the regression line. S_{res} values that are much smaller than the standard error of $\langle\Delta\delta/\Delta T\rangle$ in the first column indicate that inclusion of a CSD dependence improves the prediction of $\Delta\delta/\Delta T$ values.

To our knowledge, only two other reports have acknowledged a correlation between NH $\Delta\delta/\Delta T$ and shift deviation. Blanco et al.[33e] rationalized their observation by reference to our endothelin studies.[2c] However, Rothemund et al.[39] suggested an alternative explanation and implied that it could apply for the endothelin systems that we reported. Rothemund et al. reported data for two helical peptides in 50% aqueous TFE. They suggested that, as the temperature is lowered, TFE increasingly protonates the already intramolecularly bonded carbonyls of the peptide helix, yielding a bifurcated H-bonded state which displays a downfield shift. That could rationalize negative $\Delta\delta/\Delta T$ values for NHs which were presumably protected by a helical H-bonding network. While this rationale seems unlikely to apply to a strictly aqueous medium, it does need to be examined for aqueous fluoroalcohol media.

NH $\Delta\delta/\Delta T$ Values in Proteins and a Comparison with Less-Structured Protein Fragments. Although NMR structures have been reported for more than 100 proteins, the database of protein NH $\Delta\delta/\Delta T$ values is still rather small (even when the values are measured, the results are rarely reported). We have assembled a database of 361 NHs from proteins and highly cross-linked peptides for which chemical shifts (and their gradients) as well as exchange protection status have been determined.[16,25,28−32] On the basis of his data, it does indeed appear, for "rigid" segments of protein structure in aqueous media, that hydrogen-bonded NHs are *usually* characterized by gradients of -2.0 ± 1.4, while exposed NHs have larger negative gradients and NHs in highly disordered terminal segments have gradients of $-6 \rightarrow -8.5$. However, there are many exceptions. Figure 2 shows the complete protein data set with amides differentiated by exchange protection and hydrogen-bonding status. The complete set of $\Delta\delta/\Delta T$ averages and least-squares correlation parameters by exchange protection and structural categories appears in Table 2.

From Table 2, it is apparent that hydrogen bonding and/or exchange protection results in less negative $\Delta\delta_{NH}/\Delta T$ values. However, there is too much statistical overlap of the various catagories for gradients to be used to determine hydrogen-bonding status. For example, the −4 ppb/°C criterion previously mentioned displays a false positive rate of 34−36%, depending on whether exchange rates (or H-bonds in the NMR ensemble) are used as the criterion. Assuming that a correlation between NH shift deviation and temperature gradient could still be

(42) Chen, C. Ph.D. Thesis, University of Washington, 1992.
(43) Andersen, N. H.; Lee, G. M.; Porubcan, M. A.; Hunt, J. T.; Lee, V. G. Manuscript in preparation, presented in part at the 36th Experimental NMR Conference, Boston, MA, March 1995, Abstract P-133, p 165.
(44) (a) Reily, M. D.; Dunbar, J. B., Jr. *Biochem. Biophys. Res. Commun.* **1991**, *178*, 570−577. (b) Coles, M.; Munro, S. L. A.; Craik, D. J. *J. Med. Chem.* **1994**, *37*, 656−664. (c) Gradient were also calculated from data presented by: Ragg, E.; Mondelli, R.; Penco, S.; Bolis, G.; Baumer, L.; Guaragna, A. *J. Chem. Soc., Perkin Trans.* **1994**, *2*, 1317−1326.
(45) Xu, X.; Nelson, J. W. *Biochemistry* **1994**, *33*, 5253−5261 and references cited therein.

Table 2. (A) Least-Squares Correlations of NH Shift Deviations and Temperature Gradients for Proteins (and Highly Structured Peptides) and (B) Same Correlation for Peptides Corresponding to Protein Sequence Fragments[a]

		least-squares ($\Delta\delta/\Delta T$, CSD) correlation				
	$\langle\Delta\delta/\Delta T\rangle$ (se)	n	$\Delta\delta/\Delta T$, CSD = 0	S_{res}	slope	R
A. Proteins and Highly Structured Peptides						
protein summary	−3.88 (2.76)	361	−3.70 (0.14)	2.60	−1.18	0.34
all H-bonded	−2.75 (2.17)	172	−2.56 (0.16)	2.04	−0.92	0.35
all non-H-bonded	−4.92 (2.84)	189	−4.73 (0.19)	2.56	−1.65	0.44
slow exchanging	−2.86 (2.44)	153	−2.67 (0.20)	2.36	−0.83	0.27
H-bonded	−2.24 (1.80)	111	−2.03 (0.17)	1.69	−0.80	0.36
no H-bonding	−4.50 (3.08)	42	−4.31 (0.47)	2.97	−1.38	0.30
partially protected	−3.37 (2.43)	33	−3.30 (0.36)	2.06	−1.62	0.55
H-bonded	−3.42 (1.93)	11	−2.65 (0.46)	1.34	−2.01	0.75
no H-bonding	−3.35 (2.69)	22	−3.55 (0.51)	2.36	−1.67	0.52
fast exchanging	−4.88 (2.75)	175	−4.69 (0.19)	2.47	−1.56	0.45
H-bonded	−3.74 (2.59)	50	−3.66 (0.34)	2.37	−1.31	0.43
no H-bonding	−5.33 (2.69)	125	−5.10 (0.22)	2.39	−1.62	0.46
Statistics for Individual Proteins						
bNβD12[16]	−4.05 (2.22)	32	−3.80 (0.42)	2.18	−0.99	0.26
slow exchanging	−3.07 (1.58)	15	−2.88 (0.52)	1.61	−0.42	0.18
H-bonded	−2.70 (1.23)	11	−2.49 (0.49)	1.26	−0.44	0.22
no H-bonding	−4.10 (2.16)	4	−3.91 (1.51)	2.60	−0.43	0.17
fast exchanging	−4.92 (2.39)	17	−4.60 (0.38)	1.55	−4.07	0.78
ω-Conotoxin GVIA[29a]	−2.83 (2.48)	23	−2.73 (0.49)	2.33	−1.33	0.40
slow exchanging	−0.71 (0.49)	7	−0.74 (0.15)	0.40	−0.32	0.66
H-bonded	−2.07 (1.73)	14	−1.89 (0.44)	1.60	−1.00	0.46
fast exchanging	−3.75 (2.44)	16	−3.49 (0.57)	2.21	−1.92	0.48
H-bonded	−3.00 (1.77)	8	−2.48 (0.54)	1.39	−1.92	0.69
no H-bonding	−4.50 (2.88)	8	−4.51 (0.89)	2.53	−2.84	0.58
Cellobiohydrolase[29b]	−2.24 (3.42)	33	−1.82 (0.50)	2.83	−2.21	0.34
slow exchanging	+0.26 (1.97)	13	+0.45 (0.45)	1.60	−1.34	0.63
fast exchanging	−3.87 (3.20)	20	−3.28 (0.50)	2.19	−2.64	0.75
Leu^5-EETI-2[29c]	−5.67 (3.32)	25	−5.56 (0.67)	3.30	−1.30	0.23
slow and H-bonded	−3.27 (1.71)	8	−3.27 (0.63)	1.77	+0.63	0.28
partially protected	−4.74 (2.78)	5	−4.74 (1.42)	3.18	−0.91	0.15
fast exchanging	−7.70 (1.71)	6	−7.70 (0.87)	1.92	−0.02	0.01
BPTI[28]	−3.28 (2.15)	52	−3.23 (0.29)	2.10	−0.68	0.27
slow exchanging	−1.94 (1.19)	20	−1.83 (0.27)	1.15	−0.38	0.35
non-bonded	−1.88 (—)	1				
H-bonded	−1.94 (1.22)	19	−1.79 (0.29)	1.17	−0.43	0.36
slightly protected	−2.90 (2.02)	14	−3.41 (0.40)	1.42	−2.85	0.74
all H-bonded	−2.06 (1.26)	25	−2.01 (0.25)	1.24	−0.35	0.28
all non-bonded	−4.40 (2.23)	27	−4.40 (0.37)	1.89	−1.79	0.55
all fast exchanging	−5.07 (1.89)	18	−4.99 (0.41)	1.74	−1.16	0.45
no H-bonding	−5.54 (1.66)	15	−5.43 (0.45)	1.68	−0.55	0.23
Eglin-c[30]	−4.81 (2.54)	63	−4.62 (0.32)	2.47	−1.13	0.26
interstrand sheet	−2.92 (1.27)	12	−2.50 (0.58)	1.33	+0.84	0.29
helical, protected	−3.52 (1.82)	16	−3.63 (0.46)	1.81	−1.02	0.36
N-term. random	−7.03 (0.66)	8	−6.91 (0.33)	0.74	+0.98	0.23
remaining unprotected	−5.56 (3.09)	14	−4.94 (0.74)	2.61	−3.00	0.59
Hevein	−3.76 (2.32)	78	−3.66 (0.25)	2.15	−1.16	0.39
H-bonded by NMR	−3.33 (2.22)	41	−3.23 (0.34)	2.15	−0.84	0.29
all protected NHs	−2.88 (1.95)	38	−2.68 (0.25)	1.50	−1.49	0.66
slowest exchanging	−2.61 (1.43)	24	−2.54 (0.20)	0.97	−1.45	0.75
interstrand β sheet	−3.29 (2.01)	15	−2.17 (0.32)	1.05	−2.09	0.87
not exchange protected	−4.60 (2.33)	40	−4.57 (0.36)	2.30	−0.82	0.24
loci of change	−4.86 (2.13)	19	−4.81 (0.44)	1.93	−1.73	0.52
Interleukin-8[31]	−4.08 (3.04)	55	−3.74 (0.40)	2.84	−1.09	0.38
all slow exchanging	−2.51 (1.44)	19	−1.97 (0.38)	1.29	−0.99	0.49
H-bonded	−2.50 (1.48)	17	−1.96 (0.44)	1.37	−0.96	0.44
in β sheet	−2.95 (1.61)	10	−2.21 (1.05)	1.73	−0.81	0.28
all H-bonded by NMR	−3.36 (2.40)	33	−2.96 (0.40)	2.15	−1.19	0.47
all fast exchanging	−4.91 (3.34)	36	−4.66 (0.50)	2.96	−1.36	0.49
fast, no H-bonding	−5.43 (3.66)	20	−5.15 (0.80)	3.50	−1.08	0.37
B. Protein Sequence Fragments						
complete sets of sequence fragments						
BPTI[33c]	−7.31 (1.56)	65 (5)	−6.95 (0.13)	0.97	−8.24	0.79
plastocyanin[33b]	−6.95 (1.33)	115 (14)	−6.56 (0.10)	0.46	−5.97	0.70
myohemerythrin[33a]	−7.64 (1.81)	94 (19)	−7.51 (0.17)	1.60	−5.61	0.49
G B1-domain[33de]	−7.33 (1.12)	68 (19)	−6.94 (0.11)	0.83	−5.99	0.68
all four series	−7.08 (1.66)	399	−6.85 (0.07)	1.27	−6.44	0.64
excluding structured	−7.28 (1.51)	342	−6.98 (0.07)	1.21	−6.01	0.60
structured regions	−5.88 (1.98)	(57)	−6.18 (0.20)	1.48	−6.35	0.68
Apolipoprotein[34a]						
E(263−286)	−4.48 (3.94)	22	−6.41 (0.58)	2.31	−7.63	0.82
E(267−289)	−5.10 (2.93)	21	−6.31 (0.50)	2.00	−9.56	0.75
myelin basic protein[34b]	−6.72 (0.79)	13	−6.30 (0.31)	0.73	−4.78	0.47

[a] The format and notes of Table 1 apply.

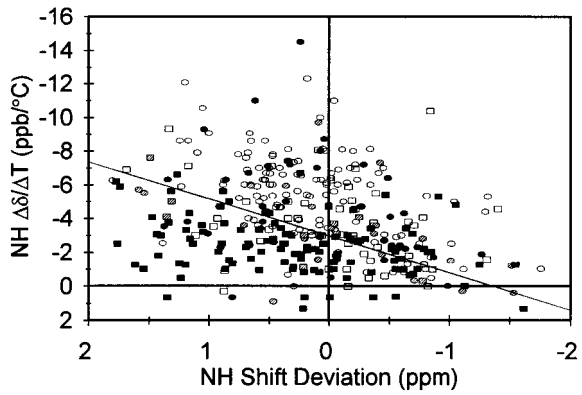

Figure 2. Amide NH CSD-$\Delta\delta/\Delta T$ correlation for 361 NHs in proteins and highly cross-linked peptides. Amide categories are labeled by the following symbol legend: fully filled, significantly exchange protected; partially filled, modestly exchange protected; open, fast exchanging; square symbols correspond to NHs that are H-bonded in the NMR structural ensemble; round symbols are non-bonded NHs. The line corresponds to $\Delta\delta/\Delta T = -2.97 - (\mathrm{CSD}\cdot 2.19)$.

present due to residual conformational averaging or the weakening of H-bonds due to increased local backbone libration upon warming yields better cutoff criteria for determining hydrogen-bonding status. Table 3 compares the false positive and negative rates for −4 ppb/°C and several other cutoff lines. One of these, a line corresponding to $\Delta\delta_{NH}/\Delta T = -4.4 - (\mathrm{CSD}\cdot 7.8)$, was derived from a study of largely unstructured protein fragments (also shown in Table 2)—97% of the data points from the protein fragments display $\Delta\delta/\Delta T$ values more negative than the cutoff line. When this same line is traced through the protein NH database, 60% of the entries lie at less negative $\Delta\delta/\Delta T$ values. Sixty four percent of the NHs lying at less negative gradient values are slow exchanging and/or were identified as hydrogen bonded in the NMR structure ensembles. The statistics for three cutoff lines that provide superior discrimination of exposed and exchange-protected NHs within the protein database are given in Table 3. In all cases, the accuracy of "sequestration" assignments based on the position of an NH on the CSD-$\Delta\delta/\Delta T$ correlation graph is significantly improved if those NHs that appear at extreme upfield positions (CSD ≤ −0.45 ppm) are excluded: 88% (92% if upfield NHs are excluded) of the points lying above the $\Delta\delta/\Delta T = -3.37 - (\mathrm{CSD}\cdot 1.8)$ line are exposed based on exchange measures and the NMR derived structure; $-2.97 - (\mathrm{CSD}\cdot 2.2)$ picks up 65% of the H-bonded NHs (68%, if the upfield NHs are excluded); the $-2.11 - (\mathrm{CSD}\cdot 2.4)$ line displays the lowest false positive rate (11−12% whether or not the upfield NHs are excluded) for detecting "NH sequestration". For the latter, NHs are considered "unsequestered" if they do not display either 20-fold protection from exchange or an intramolecular H-bond in the NMR structure ensemble.

We do not, however, recommend the use of any of these criteria for determining whether protein NHs are slow-exchanging; making verifiable assumptions is never warranted. But it is clear that, once the dependence of $\Delta\delta_{NH}/\Delta T$ values upon chemical shift is recognized, the gradients do provide structural insights for proteins and relatively rigid peptides even in the absence of NH exchange protection data. This conclusion does not apply to peptides that display certain types of conformational averaging (*vide infra*).

There have been four notable studies in which the shifts and temperature gradients of NH resonances for a set of fragments that correspond to a complete protein (or domain) have been systematically evaluated.[33] The sequence fragments are of relatively short length (11 ± 5 residues, for 40 fragments) and

Table 3. Statistics for the Detection of Exchange Protected and H-Bonded Amide NHs in Proteins using Different Cutoff Lines through the CSD/Gradient Plot[a]

	slow		med		fast		
	HB	no HB	HB	no HB	HB	no HB	all
A. Complete 361 Point Data Set							
$-4.4 - 7.8\cdot$CSD							
above	31	22	2	12	21	58	146
below	80	20	9	10	29	67	215
−4							
above	17	20	4	8	18	86	153
below	94	22	7	14	32	39	208
$-3.37 - 1.79\cdot$CSD							
above	18	24	3	11	25	98	179
below	93	18	8	11	25	27	182
$-2.97 - 2.19\cdot$CSD							
above	28	28	4	12	29	102	203
below	83	14	7	10	21	23	158
$-2.11 - 2.41\cdot$CSD							
above	46	32	7	16	37	118	256
below	65	10	4	6	13	7	105
B. Excluding 74 Upfield NHs with CSD < −0.45							
$-4.4 - 7.8\cdot$CSD							
above	7	9	1	6	11	38	72
below	79	20	9	10	29	68	215
−4							
above	14	17	4	8	15	82	140
below	72	12	6	8	25	24	147
$-3.37 - 1.79\cdot$CSD							
above	8	17	3	9	20	88	145
below	78	12	7	7	20	18	142
$-2.97 - 2.19\cdot$CSD							
above	16	17	4	9	23	89	158
below	70	12	6	7	17	17	129
$-2.11 - 2.41\cdot$CSD							
above	23	19	6	11	29	100	188
below	63	10	4	5	11	6	99

[a] The number of NHs appearing above and below each possible cutoff line is tabluated.

thus should provide baselines for both minimally and partially structured peptides. In Figure 3, we have labeled sites that were shown, based on NOE ratios or medium-range NOE occurences,[46] to have some structure in aqueous media; the individual correlations appear in Table 3. The correlation of the data in Figure 3 predicts a random coil gradient of 7.0 ppb/°C, and the correlation coefficient ($R = 0.64$) is essentially unaltered by excluding the sites that are partially structured. In fact, the 57 excluded data points displayed a slightly better correlation ($R = 0.68$).

The peptide fragment data set (Figure 3) does not contain points in the lower left-hand corner of the correlation plot. This location in a CSD-$\Delta\delta/\Delta T$ correlation plot appears to be a near conclusive indicator of persistent hydrogen-bond formation. In fact, all of the sequence fragment data points with NH CSD ≥ −0.5 ppm have $\Delta\delta/\Delta T$ values more negative than the cutoff line which provides the best definition of hydrogen-bond formation in the protein database (this line is shown in both Figures 2 and 3). The dashed line on Figure 3 represents the least negative $\Delta\delta/\Delta T$ values that can be expected for the exposed NHs of minimally structured peptides.

Overall, the gradient data for proteins and rigid peptides shows much less correlation with NH shift deviation; the residual correlations display much smaller slopes than is observed in the endothelin/apamin analogues and protein fragments. The only categories that tend to display a significant gradient/CSD

(46) Although a number of the authors used NH temperature gradients to confirm loci of structuring, our exclusions of NH points appearing in Figure 3 from the correlation shown in Table 2 were based only on NOE and scalar coupling observations.

correlation slope are the partially protected NHs and those that are not H-bonded. This suggests that structuring which produces chemical shift deviations from random coil values and is easily lost with increasing temperature, yields the best NH $\Delta\delta/\Delta T$-CSD correlations. Several temperature-influenced phenomena can be suggested, for example, side chain rotamer equilibration and backbone segmental motion. These could increase significantly on warming, even at temperatures well below the melting temperature of the protein.

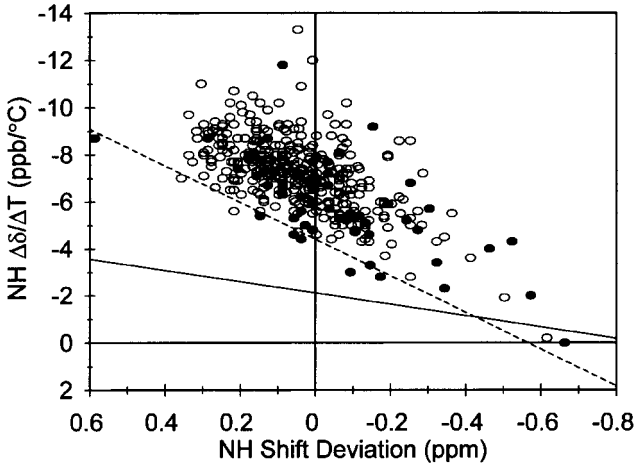

Figure 3. Amide NH CSD-$\Delta\delta/\Delta T$ plot for protein fragments (399 points). The 57 points, which correspond to sites that were reported to display nonaveraged $J_{N\alpha}$ couplings and medium-range NOEs indicative of structuring, are shown in black while the open circles are presumably unstructured NHs. The dashed line corresponds to $\Delta\delta/\Delta T = -4.4 -$ (CSI·7.8). The $-2.11 -$ (CSD·2.4) line, which provided the best differentiation of sequestered NHs in the protein database (Figure 2) is also shown.

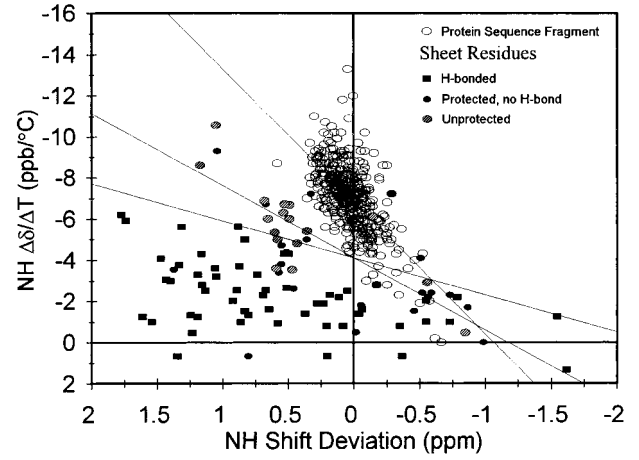

Figure 4. Comparison of the data points for protein fragments and protein β-sheet regions. The hydrogen-bonded sites within the protein sheet regions all lie below the $\Delta\delta/\Delta T = -4.1 -$ (CSD·1.8) line which is shown. The least-squares fit for the protein fragment data, $\Delta\delta/\Delta T = -6.85 -$ (CSD·6.4) ($R = 0.64$), and for the unprotected NHs of the protein sheet region, $\Delta\delta/\Delta T = -4.11 -$ (CSD·3.5) ($R = 0.79$), are also shown.

To support our contention that conformational averaging is the major source of deviant values of $\Delta\delta_{NH}/\Delta T$, we present a comparison (Figure 4) of the data points reflecting the most rigid β-sheet cores of the proteins ($n = 95$) and the data for 399 NHs from the distinctly nonrigid sequence fragments. Within the rigid β-sheet cores of proteins there are both NHs that have interstrand H-bonds and externally directed NHs; however, nearly all of the NH temperature gradients lie at less negative $\Delta\delta/\Delta T$ values than the points for the sequence fragments. The fragments show a much greater range of $\Delta\delta/\Delta T$ values and a significant correlation with NH shift deviation. It is also of interest that the fast exchanging NHs in the protein β sheets, for which no hydrogen bonds were found, display a correlation with NH shift deviation ($R = 0.79$). This suggests that the factors which influence shift for these NHs, presumably solvent interactions *and* the spatial disposition of side chain groups, are temperature dependent. The NH resonances of the solvent-exposed β-sheet residues are shifted downfield of their expected value (based on the protein fragment data) as a result of the approximately 0.3 ppm secondary structure shift contribution associated with β-sheets.[3g] Exchange-protected amides for which no H-bonds were identified have little correlation with NH-CSD and have a large range of NH $\Delta\delta/\Delta T$ values.

NH Temperature Gradients as a Measure of Structuring in Linear Peptides. We will now examine linear peptides (Table 4) with well-defined structuring tendencies to illustrate some of the information found in an NH CSD-$\Delta\delta/\Delta T$ correlation plot when a temperature-dependent structured → coil state equilibrium is present. Two peptide fragments from protein G B1 that correspond to a helical and a β-hairpin section of the native structure will be considered. This will be followed by an examination of a salmon calcitonin fragment. This fragment displays, in aqueous fluoroalcohol, one well-defined helix which does not encompass the entire sequence; the rest of the residues remain disordered. These and other partially structured peptides provide insights into the NH CSD-$\Delta\delta/\Delta T$ correlation and evidence for the importance of temperature-dependent equilibria as the primary determinants of NH temperature gradients.

In their examination of the protein G B1 domain fragments, Blanco and Serrano found that the helix fragment (21−40) and the C-terminal β-hairpin fragment (41−56) increasingly formed the native secondary structure upon addition of TFE.[33e] These are also the first structural elements observed in pulsed H-D exchange studies of the protein G refolding reaction[47] and, not coincidentally, the two fragments which give the best NH CSD-$\Delta\delta/\Delta T$ correlation. These two fragments show an unusually wide range of gradient values which increases upon TFE addition; in 30% TFE, the helical fragment displays $\Delta\delta_{NH}/\Delta T$ values of $+6.6 \rightarrow -15.5$ while the β-hairpin (Figure 5) displays the widest range of gradient values which we have found in the literature, $+10.8 \rightarrow -26$ ppb/°C. We attribute the increased range of NH shift deviations to the increased population of the native secondary structures at lower temperatures.

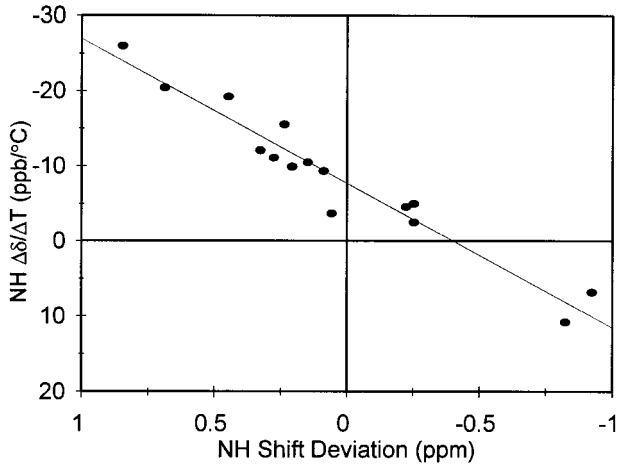

Figure 5. Amide NH CSD-$\Delta\delta/\Delta T$ correlation for the residue 41−56 fragment of the B1 domain of protein G in 30% aqueous TFE.[33e] The correlation coefficient for the least-squares line (slope = −19.06 ppt/°C) shown is $R^2 = 0.95$.

Table 4. Least-Squares Correlations of NH Shift Deviations and Temperature Gradients for Partially Structured Peptides[a]

		least-squares ($\Delta\delta/\Delta T$, CSD) correlation				
	$\langle\Delta\delta/\Delta T\rangle$ (se)	n	$\Delta\delta/\Delta T$, CSD = 0	S_{res}	slope	R
Peptides in Aqueous Media						
nascent helices						
G-B1(21−40)[33e]	−6.85 (1.14)	19	−6.85 (0.25)	1.10	−4.18	0.40
myoheme(1−18)[33a]	−7.64 (3.63)	14	−9.59 (0.89)	2.68	−12.20	0.73
myoheme(18−38)[33a]	−6.84 (1.95)	20	−7.08 (0.36)	1.56	−7.39	0.65
Annexin I fragment[34c]	−5.97 (1.65)	20	−6.27 (0.30)	1.27	−6.61	0.66
myoglobin H helix[34d]	−5.76 (1.98)	27	−6.48 (0.40)	1.71	−7.54	0.53
designed helices						
Bradley et al.[37a]	−5.00 (5.88)	17	−7.59 (0.75)	2.76	−20.47	0.90
Merutka et al.[37b]	−1.50 (2.73)	17	−6.43 (0.58)	1.10	−15.27	0.93
β-hairpin fragments						
tendamistat[35a]						
12−26	−6.14 (1.82)	14	−7.27 (0.29)	0.88	−7.74	0.89
15−23	−6.26 (1.87)	8	−7.65 (0.54)	1.11	−7.76	0.84
[S18] 15−23	−7.04 (1.11)	8	−7.13 (0.24)	0.68	−5.99	0.82
Barnase 96−110[35b]	−5.86 (1.41)	14	−5.91 (0.20)	0.76	−9.77	0.85
G-B1(41−56)[33e]	−6.66 (1.80)	15	−6.51 (0.35)	1.33	−8.36	0.73
designed β-hairpins[36]						
peptide 1[36a]	−6.24 (2.48)	7	−6.14 (0.84)	2.21	−5.99	0.58
peptide 2	−6.30 (2.42)	8	−7.03 (0.36)	0.96	−8.89	0.93
peptide 3	−6.19 (3.21)	9	−6.72 (0.49)	1.44	−12.38	0.92
peptide 4	−6.00 (2.57)	9	−6.56 (0.47)	1.37	−9.04	0.87
peptide 5	−6.10 (1.71)	8	−6.65 (0.35)	0.93	−6.49	0.88
peptide 6	−5.92 (1.84)	9	−6.51 (0.27)	0.76	−7.30	0.93
peptide 7	−6.03 (2.08)	9	−6.30 (0.61)	1.77	−3.29	0.60
Peptides in Aqueous Fluoroalcohol						
helix forming systems						
G-B1(21−40)[33e]	−6.31 (5.61)	19	−7.56 (0.19)	3.24	−19.31	0.84
sCTF (8−32)	−5.04 (1.57)	22	−6.11 (0.25)	0.89	−5.93	0.84
helix (11−22)	−4.39 (1.71)	12	−6.01 (0.24)	0.58	−6.65	0.95
remainder	−5.54 (0.79)	8	−5.78 (0.28)	0.70	−2.51	0.57
Pramlintide	−4.88 (2.76)	33	−5.31 (0.28)	1.56	−5.61	0.83
unfolding helix (8−20)	−5.89 (2.89)	13	−5.46 (0.31)	1.09	−5.64	0.93
C-terminus (23−37)	−4.76 (0.89)	12	−4.88 (0.35)	0.92	−0.60	0.17
RNACP-1						
4% HFIP	−4.66 (5.22)	12	−8.25 (0.80)	2.21	−14.50	0.92
10% HFIP	−4.37 (3.48)	12	−6.69 (0.36)	1.02	−10.39	0.96
21% HFIP	−4.63 (3.06)	12	−6.42 (0.29)	0.87	−8.57	0.97
other helical peptides[38]						
PH 1.0	−4.42 (2.56)	11	−5.52 (0.44)	1.28	−7.88	0.88
PH 1.12	−4.01 (1.86)	11	−4.69 (0.37)	1.11	−4.69	0.82
PH 1.13	−5.46 (2.17)	11	−6.01 (0.56)	1.72	−4.61	0.66
PH 1.19	−5.46 (2.17)	11	−6.01 (0.56)	1.72	−4.61	0.66
PH 1.4	−4.56 (2.42)	11	−5.44 (0.41)	1.25	−7.95	0.87
Rothemund et al.[39]						
LA18	−4.64 (2.05)	18	−5.06 (0.22)	0.90	−6.41	0.91
LN18	−6.95 (2.13)	18	−6.16 (0.40)	1.49	−6.29	0.74
β-hairpin forming system						
G-B1(41−56)[33e]	−8.81 (9.41)	15	−7.82 (0.68)	2.62	−19.06	0.97
other protein sequence fragments						
Annexin I fragment[34c]	−5.43 (2.03)	19	−6.46 (0.47)	1.60	−7.95	0.64
CI2 frag 1−28[34f]	−4.59 (2.00)	20	−4.66 (0.31)	1.38	−5.22	0.74
Staphylococcal nuclease[34e]	−7.25 (2.92)	13	−8.06 (0.75)	2.44	−10.00	0.60

[a] The format and notes of Table 1 apply.

These two peptides have excellent NH CSD-$\Delta\delta/\Delta T$ correlation coefficients and large slopes in 30% TFE (see Table 4 and Figure 5). This behavior is not restricted to aqueous fluoroalcohol media. We have found a number of literature cases[37] (included in Table 4) of similar correlation for the thermal melting of helices in purely aqueous medium; others have been observed in this laboratory. We contend that the correlation of CSD and $\Delta\delta/\Delta T$ values observed for all of these systems provides compelling evidence that essentially all of the NH shift deviation from reference values is due to the concerted formation of a single structured state on cooling. A steep slope for the correlation reflects facile thermal melting of the folded state. The correlation for the protein G B1(41−56) β hairpin also supports our hypothesis; β-hairpin formation is, of necessity, a cooperative structuring transition.

To further probe the relationship between $\Delta\delta/\Delta T$ values and NH-CSDs, we have examined some peptides (Table 4) that lack disulfide cross-linking and display classic helix/coil equilibria based on both NMR and CD spectroscopy. The first of these is an analogue of salmon calcitonin[48] (sCTf). In aqueous buffer throughout the pH range 2.5−8, sCTf displays only a very weak shoulder near the expected n → π^* minimum of an α-helix in

(47) Kuszewski, J.; Clore, G. M.; Gronenborn, A. M. *Protein Sci.* **1994**, *3*, 1945−1952.

(48) (a) Structure of calcitonin in methanol: Meadows, R. P.; Nikonowicz, E. P.; Jones, C. R.; Bastian, J. W.; Gorenstein, D. G. *Biochemistry* **1991**, *30*, 1247−1254. (b) Xaa-Pro isomers in DMSO: Amodeo, P.; Antonietta, M.; Morelli, C.; Motta, A. *Biochemistry* **1994**, *33*, 10754−10762. (c) N^{α}-acetyl-sCT(8-32)-NH_2 is reported to be a potent antagonist: Feyen, J. H. M.; Cardinaux, F.; Gamse, R.; Bruns, C.; Azria, M.; Trechsel, U. *Biochem. Biophys. Res. Commun.* **1992**, *187*, 8−13.

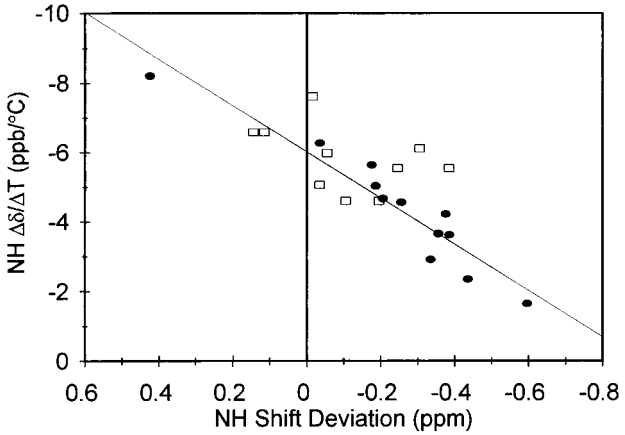

Figure 6. Amide NH CSD-$\Delta\delta/\Delta T$ correlation for sCTf(8−32) in aqueous HFIP. The NHs in the helical segment are shown as filled circles, the remainder as unfilled squares. The line is the least-squares fit for the helical NHs: $R^2 = 0.91$, slope = −6.65 ppt/°C.

the CD spectrum. This ellipticity, $[\theta]_{219} = -1740-32\cdot T$ (°C), becomes more positive upon cooling as previously noted for other coil state peptides which gain polyPro$_{II}$ structure upon cooling.[49] Both the αH conformational shifts and the inter/intraresidue αN NOE ratios[19,22a] indicate a random coil state with "averaged" $\alpha_i N_{i+1}$ distances that are dominated by the short distances associated with extended Ψ values. In 25 vol % HFIP, sCTf has an end-frayed, but otherwise well-defined, helical segment $\{[\theta]_{221} = -14600 + 86\cdot T$ (°C)$\}$ from Gly^{10} to Tyr^{22} based on the observed αH-CSDs and inter/intraresidue αN NOE ratios (see Supporting Information).

In 25% HFIP, sCTf displays a rather wide range of NH temperature gradients, $\Delta\delta/\Delta T = -8.6$ to -1.4, with both extremes recorded for NHs that would be expected to be at least somewhat protected by a helical H-bonding network. The NH CSD-$\Delta\delta/\Delta T$ correlation plot appears as Figure 6. We view the excellent linear correlation in the helical domain ($R = 0.95$), as a confirmation that a two-state helix/coil transition occurs for sCTf. The least-squares line for the NHs from the remainder of the sequence has a much reduced slope and a low correlation coefficient ($R = 0.57$). Pramlintide, which also has a single-helical segment that does not encompass the complete sequence, also has a steeply sloped CSD-$\Delta\delta/\Delta T$ correlation only over the helical segment (see Table 4).

The C-peptide of bovine pancreatic RNase-A is the first discovered[50] and most thoroughly studied short helical peptide.[51] Analogues of this sequence were chosen for a more detailed study of the effect of fluoroalcohol upon NH shifts and gradients. Although the structural features that produce the surprisingly large helical propensity for the C-peptide sequence have been extensively studied by both NMR and CD, the present studies have yielded some correlations that had not been noted previously. These are illustrated with peptide RNACP-1. The changes in αH-CSD values during a fluoroalcohol titration at 262 K are shown in the upper panel of Figure 7. The αH-CSD histograms reveal increased helicity, particularly at the extreme ends, upon increasing the HFIP content and (data not shown) upon cooling. The corresponding plot of NH-CSD histograms (lower panel) is quite interesting. The increase in helicity during

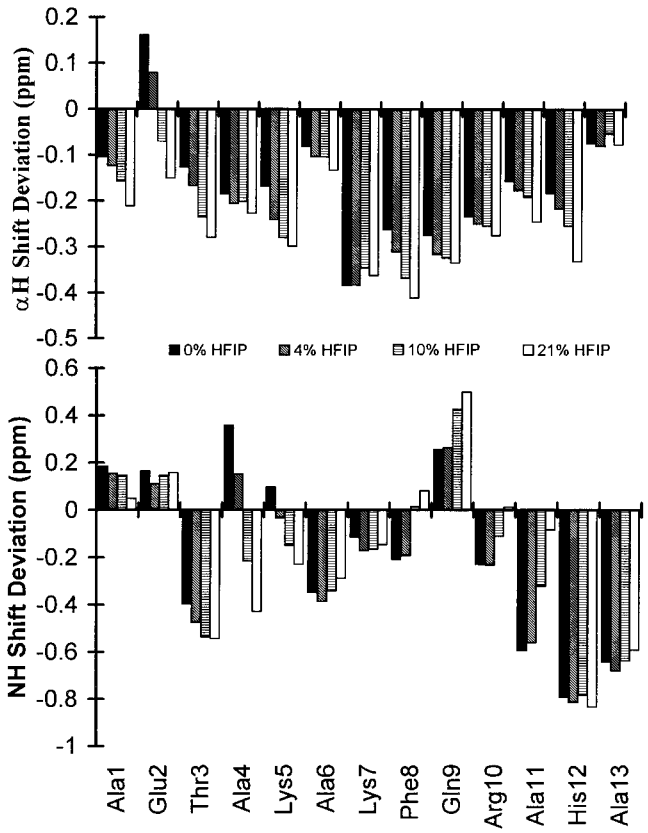

Figure 7. Changes in αH chemical shift deviations of peptide RNACP-1 during a fluoroalcohol titration to increasing helicity. The data for 0, 4, 10, and 21% HFIP are shown, left to right, at each residue: upper panel, αH-CSD histograms; lower panel, NH-CSD histograms. The random coil values were corrected for the HFIP content of the medium and the temperature as described in the Materials and Methods.

the HFIP titration is accompanied by dramatic changes, even sign changes, in NH-CSD values. Nonetheless, at each solvent composition, the NH chemical shift deviations uniformly move toward zero with increasing temperature at every NH from residue Thr^3 through Ala^{13} when the NH reference values are corrected for temperature using a uniform −7.6 ppb/°C correction.[6a] This suggests that loss of helicity occurs throughout the helical span. The temperature effect at 21% HFIP is shown in Figure 8.

The range of NH CSD values increases with increased helicity while the range of $\Delta\delta/\Delta T$ values decreases: +5.0 → −13.6 (4% HFIP), +1.8 → −10.7 (10% HFIP), +1.3 → −9.4 ppb/°C (21% HFIP). The positive gradients are associated with the NHs of the residues at the C-terminus of the helix which are shifted far upfield, presumably by the helix macrodipole interaction.[3d] The corresponding NH-CSD/gradient correlation plots appear as Figure 9. The NH temperature gradients at each HFIP level correlate with the NH-CSD values. The correlation even holds for Ala^4, Lys^5, and Ala^{11}, the three residues which display dramatic changes in their CSD values during the HFIP titration—as an example Ala^4 has a gradient of −13.6 when it appears at 8.64 ppm (4% HFIP) and a much diminished gradient of −2.1 ppb/°C when it appears at 8.05 ppm (21% HFIP). The R value increases as the HFIP level in the medium increases. This improvement in fit is best measured as the rms residual in $\Delta\delta/\Delta T$ prediction which drops from 2.21 to 0.87 ppb/°C as the HFIP content is increased.

In our view, this correlation has a number of implications with regard to both the nature of the structuring transition of this C-peptide analogue and the quantitative relationship between

(49) Woody, R. W. *Adv. Biophys. Chem.* **1992**, *2*, 37−79.
(50) (a) Brown, J. E.; Klee, W. A. *Biochemistry* **1971**, *10*, 470−476. (b) Kim, P. S.; Baldwin, R. L. *Nature* **1984**, *307*, 329−334.
(51) See, for examples ref 24 and (a) Shoemaker, K. R.; Kim, P. S.; Brems, D. N.; Marqusee, S.; York, E. J.; Chaiken, I. M.; Stewart, J. M.; Baldwin, R. L. *Proc. Natl. Acad. Sci. U.S.A.* **1985**, *82*, 2349−2353. (b) Osterhout, J. J., Jr.; Baldwin, R. L.; York, E. J.; Stewart, J. M.; Dyson, H. J.; Wright, P. E. *Biochemistry* **1989**, *28*, 7059−7064. (c) Dtrehlow, K. G.; Robertson, A. D.; Baldwin, R. L. *Biochemistry* **1991**, *30*, 5810−5814.

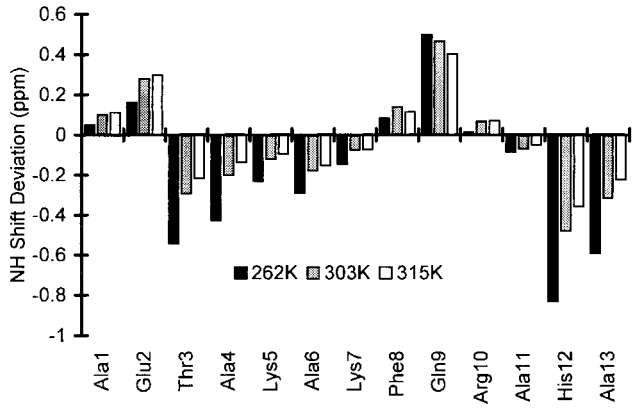

Figure 8. Effect of temperature upon the NH chemical shift deviation histogram of RNACP-1 in 21% HFIP. The random coil values for each residue were adjusted to each temperature of observation, assuming $(\Delta\delta/\Delta T)\mathrm{rc} = -7.6$ ppb/°C, prior to subtracting this value from the observed NH shift. Loss of structure is evident at all sites within the helix independent of the sign of the the NH CSD.

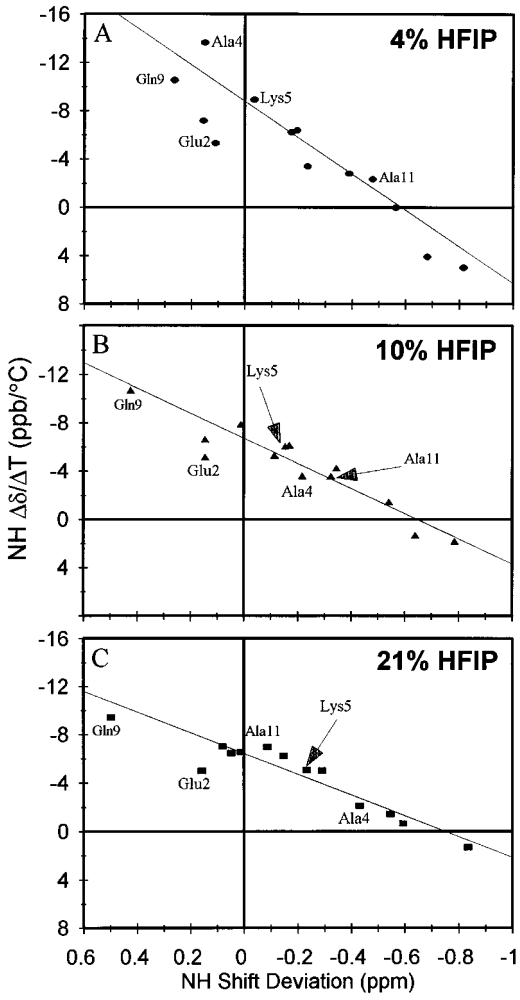

Figure 9. Amide NH CSD-$\Delta\delta/\Delta T$ correlation for C-peptide analogue RNACP-1 at three different levels of added HFIP: top panel, 4% HFIP; middle panel, 10% HFIP; lower panel, 21% HFIP; the correlation coefficient, slope and intercept of the least squares line (excluding Glu[2] from the fit) are shown in Table 4. The HN-CSI values employed for the plots are those observed at the lowest temperature examined (262 K).

temperature gradients and conformational equilibrium changes. The deviation of NH chemical shift from random coil values reflects the population of, and degree of structuring (including the strength of hydrogen bonds) in, the folded state. From the results reported herein, it appears that NH shift deviations are predominantly due to intermediate range order rather than the individual residue ϕ/Ψ values. The loss of intermediate range order for a peptide with a single secondary structure motif that encompasses the entire sequence is cooperative. As the amount of HFIP is increased, the structured portion of the helix extends over a greater portion of the sequence and thermal loss of helicity (and the folding induced shift deviations) increasingly occurs to a comparable extent over the peptide sequence from Thr[3] → Ala[13]. The contrasting behavior (see Figure 8) for Ala[1] and Glu[2] suggests that Glu[2] serves as an N-cap in the partially unfolded states that occur increasingly at higher temperatures.

Conformational Equilibria Models that Rationalize the Linearity of δ_{NH} versus Temperature Plots. Many peptides show, within experimental error, a strictly linear dependence of δ_{NH} on temperature over 30−40 °C ranges centered about ambient conditions.[13b,52] In some cases,[53] deviations in linearity have been noted; these have been rationalized as the consequence of either the intrinsic temperature dependence of chemical shifts for the structured state or a temperature-induced conformational transition. (A reviewer noted that "temperature-dependent conformational changes usually lead to a nonlinear dependence of chemical shifts with temperature.") In contrast, we are suggesting that temperature-induced changes in the population of the folded state are the major contributor to the observed NH shift temperature gradient for partially structured peptides. A shift toward increasing population of the disordered random coil state with increasing temperature should certainly yield a monotonic change in δ_{NH}, but can this model rationalize linear rather than sigmoidal plots?

The model is very simple: the conformational equilibrium of a peptide is viewed as a single ordered structure (S) in equilibrium with the fully disordered coil state. At any particular temperature, the observed chemical shifts are population weighted averages.

$$\delta_{obs} = f_S\delta_S + (1 - f_S)\delta_{rc} \quad (1)$$

At a reference temperature (T^*), all chemical shift deviations from the random coil reference values, $(\mathrm{CSD})_{obs} = f_S^*(\mathrm{CSD})_S$, are attributed to the contribution of the structured state. The structure-induced chemical shift deviations that would be observed for the pure isolated structured state are designated as $(\mathrm{CSD})_S$.

$$\delta_{obs}(T^*) = \delta_{rc}^* + f_S^*(\mathrm{CSD})_S \quad (2)$$

Assuming that the coil and structured state each display linear temperature gradients, the NH chemical shifts at some higher temperature, $T = T^* + \Delta T$, which has produced a different population of the structured state, $f_S = f_S^* + \Delta f_S$, will be given by eq 3. We define Δgrad as the difference between the intrinsic

$$\delta_{obs}(T) = \delta_{obs}(T^*) + [(\Delta\delta/\Delta T)_{rc} + f_S^*(\Delta\mathrm{grad})]\Delta T + \Delta f_S(\mathrm{CSD})_S + \Delta f_S(\Delta\mathrm{grad})\Delta T \quad (3)$$

gradients of the structured and coil states, $\Delta\mathrm{grad} = (\Delta\delta/\Delta T)_S - (\Delta\delta/\Delta T)_{rc}$. Given that the intrinsic NH temperature gradients (and Δgrad) are in the parts per billion range while structure induced shift deviations are in the parts per million range, the third term will be a significant contributor to the temperature dependence of δ_{NH}. If this model applies, a nearly linear

(52) Reed, J.; Hull, W. E.; von der Lieth, C.-W.; Kübler, D.; Suhai, S.; Kinzel, V. *Eur. J. Biochem.* **1988**, *178*, 141−154.

(53) (a) Storrs, R. W.; Truckses, D.; Wemmer, D. E. *Biopolymers* **1992**, *32*, 1695−1702. (b) Delepierre, M.; Larvor, M.-P.; Baleux, F.; Goldberg, M. E. *Eur. J. Biochem.* **1991**, *201*, 681−693.

dependence of δ_{NH} upon temperature requires a linear decrease in the population of the structured state upon warming. The fourth term in eq 3 introduces a slight and predictable curvature into the plots under specific conditions; these have been confirmed experimentally in this laboratory and in literature reports.[53a] The conditions required for a linear increase in the mole fraction of the disordered coil state on warming have been examined for both two-state folding phenomenon and for helix/coil transitions.

As previously noted, in the case of β-hairpin/coil transitions, the structuring transition should be cooperative and can, thus, be modeled as a two-state phenomenon: structure (S) $\rightarrow$ (U) unfolded, disordered.

For these analyses we employ the usual assumption[54] that ΔH_U shows a linear dependence on temperature, $\Delta H_U(T) = \Delta H_U^\circ + (T - T^\circ)\Delta Cp_U$, with T° set to 110 °C. The same temperature was used as an approximation for the entropic convergence temperature. All current models of polypeptide structuring transitions suggest that ΔS_U° should be at least 16 J K^{-1} per ordered residue in the structured state even after taking into account the negative ΔS contribution of polar backbone solvation.[55] Assuming that a cooperative folding unit involves at least five residues, thermodynamic parameters that predict a nearly linear increase in the coil state population were derived (Figure 10, panels A and B); the resulting ΔH_U° and ΔCp_U values are not exceptional. These two panels of Figure 10 show the predicted temperature dependence of the disordered coil state population calculated for two-state transitions with ΔS_U° set to 90 and 140 J K^{-1}/mol, respectively. The ΔH_U° values, adjusted to afford a f_S value of *ca.* 0.35 at ambient temperature, corresponded to *ca.* −5.2 kJ/ordered residue, 90% of typical per-residue value from studies of the thermodynamics of protein unfolding.[56,57]

For helix/coil transitions a strict two-state model is not appropriate. We have, instead, employed our recent modification[58] of Lifson−Roig helix/coil transition model which equates the propagation parameter (w) with a microscopic equilibrium constant,

$$RT \ln w = +\Delta H_U^\circ - T\Delta S_U^\circ + \Delta Cp_U[T - T^\circ - T \ln (T/T^\circ)] \quad (4)$$

in helix/coil transition simulations for determining what "conditions" would be required to predict a nearly linear increase in $\chi_{coil} \approx (1 - \langle f_H \rangle)$ with temperature. Panel C of Figure 10 shows the predicted temperature dependence of χ_{coil} from a simulation for a helix of 14-residue length; a strictly linear relationship is shown by the points. The approximation to linearity is even better in the helix/coil simulations that employ equilibrium constants at the residue level. This should not come as a surprise given the common observation that $-[\theta]_{222}$, the most common measure of helicity, decreases linearly on warming over very large temperature ranges.[59,60] The requirements for a nearly linear decrease in χ_{coil} are not unusual. With ΔS_U° taking on values of 18 ± 3 J K^{-1}/res, nearly linear plots for 10−16 residue helices requires ΔCp_U values of 25 ± 8 J K^{-1}/res and ΔH_U° values that correspond to an average of somewhat less than one H-bond per residue in the structured state. For the simulation in panel C, ΔH° is 6.1 kJ/residue, which (based on Murphy and Gills value for the average H-bond interaction in a protein[57]) corresponds to 11 H-bonds for the 14-residue helix. The ΔCp value required for linearity is not that exceptional; Shalongo et

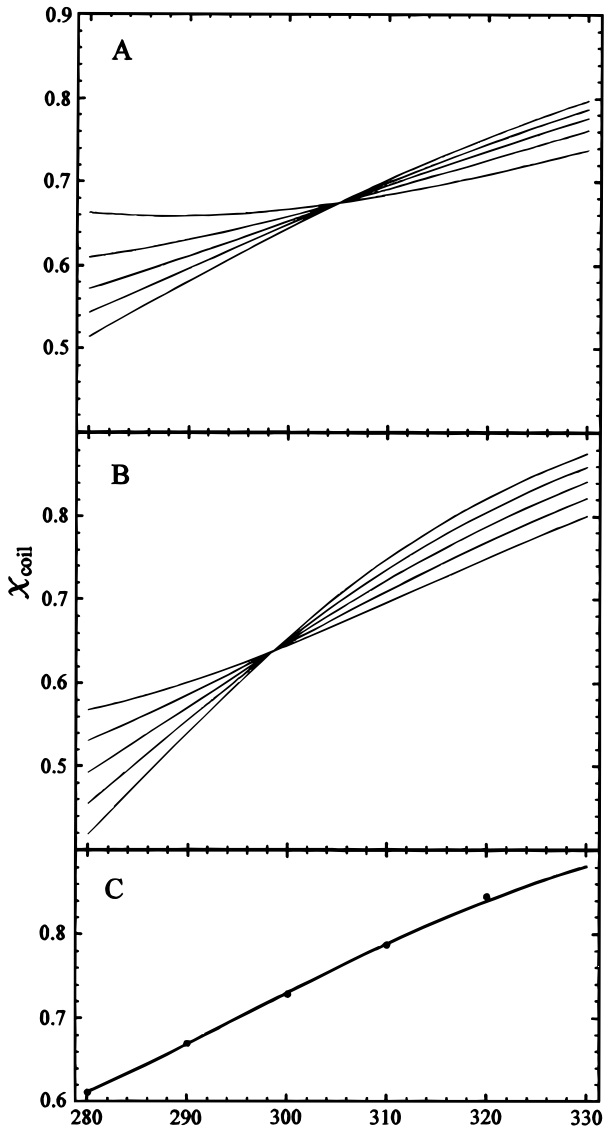

Figure 10. Simulations of the χ_{coil} dependence on temperature. Panels A and B correspond to to a two-state calculation using the equation, $-RT \ln \Delta G_U = \Delta H_U^\circ - T\Delta S_U^\circ + \Delta Cp_U[T - T^\circ - T \ln (T/T^\circ)]$: (A) Approximates a five-residue structuring feature with ΔS_U° set to 90 J K^{-1}/mol, the five lines in order of increasing slope correspond to ΔCp_U = 60, 90, 120, 160, and 220 J K^{-1}/mol, the ΔH_U° values required to have χ_{coil} = 0.68 at 305 K increases uniformly from 26.2 to 27.8 kJ/mol: (B) Approximates a nine-residue strucural feature with ΔS_U° set to 140 J K^{-1}/mol, the five lines in order of increasing slope correspond to ΔCp_U = 60, 110, 160, 210, and 260 J K^{-1}/mol, the ΔH_U° values required to have χ_{coil} = 0.64 at 298 K increases uniformly from 41.1 to 43.5 kJ/mol. Panel C is for a helix/coil transition of $GX_{14}NH_2$ with G and NH_2 having their usual N- and C-capping propensities;[58b] X is given the nucleation value of alanine with w defined by eq 4. The line in panel C was calculated with ΔH_U° = 6.1 kJ/res, ΔS_U° = 17 J K^{-1}/res and ΔCp_U = 28.7 J K^{-1}/mol. The points show a fully linear relationship of χ_{coil} with temperature over the range 280−320 K.

(54) (a) Privalov, P. L. *Adv. Prot. Chem.* **1979**, *33*, 167−241. (b) Becktel, W. J.; Schellman, J. A. *Biopolymers* **1987**, *26*, 1859−1877. (c) Privalov, P. L. *Crit. Rev. Biochem. Mol. Biol.* **1990**, *25*, 281−305.

(55) Makhataddze, G. I.; Privalov, P. L. *Protein Sci.* **1996**, *5*, 507−510.

(56) Murphy, K. P.; Freire, E. *Adv. Prot. Chem.* **1992**, *43*, 313−361.

(57) Murphy, K. P.; Gill, S. J. *J. Mol. Biol.* **1991**, *222*, 699−709.

(58) (a) Andersen, N. H.; Cort, J. R.; Liu, Z.; Sjoberg, S. J.; Tong, H. *J. Am. Chem. Soc.* **1996**, *118*, 10309−10310. (b) For further details of the calculations used in this helix/coil model, see: Andersen, N. H.; Tong, H. *Protein Sci.* **1997**, *6*, in press.

(59) Rothemund, S.; Beyermann, M.; Krause, E.; Krause, G.; Bienert, M.; Hodges, R. S.; Sykes, B. D.; Sönnichsen, F. D. *Biochemistry* **1995**, *34*, 12954−12962.

(60) The range over which a linear relationship between $-[\theta]_{222}$ and temperature is observed is even greater in aqueous fluoroalcohol media. Ranges as large as −60 to +60 °C have been observed: Merutka, G.; Stellwagen, E. *Biochemistry* **1990**, *29*, 894−898.

al. have reported values approaching 20 J K^{-1} per residue for a helical peptide.[61] In aqueous fluoroalcohol media we have documented much larger values.[58a] For both the macroscopic two-state model and in the helix/coil model, an approximately linear δ_{NH} temperature dependence is predicted only when ΔCp_U is positive and approximately 1.5 times as large as $\Delta S_U°$.

If a significant portion of the linear thermal dependence of NH resonances is, as we suggest for many peptides, the result of thermal unfolding to a coil state, the linearity observed suggests that peptides which display a significant structural preference owe this at least in part to the hydrophobic effect which is reflected in the positive ΔCp values. For polypeptides that are fixed in a single-conformational energy well throughout the temperature range examined, the $\Delta\delta_{NH}/\Delta T$ value must reflect either diminished deshielding due to intramolecular H-bonding (increased vibration amplitudes?) or desolvation upon warming. In the latter case, as well, a $T\Delta S$ term alone would yield a dependence that is not as linear as is routinely observed. Is peptide desolvation also characterized by a significant positive ΔCp?

Equation 3 also provides insights into the NH CSD-$\Delta\delta/\Delta T$ plots that we have employed for our analyses. If we assume that the structure loss is linear with temperature, $f_S(T) = f_S* + k\Delta T$, an explicit expression for the gradient can be derived, eq 5. Equation 5 provides both the slope and intercept of an NH CSD-$\Delta\delta/\Delta T$ plot.

$$\partial\delta_{NH}/\partial T = [(\Delta\delta/\Delta T)_{rc} + f_S*(\Delta\text{grad})] + 2k\Delta T(\Delta\text{grad}) + k(\text{CSD})\text{s} \quad (5)$$

The slope of the correlation plot will be considered first. Recalling that our plot is based on the observed chemical shift deviations at the low reference temperature, not upon $(CSD)_S$, the slope of the correlation plot is given by $m = k(f_S*)^{-1}$. The partially structured peptides which are most profitably examined using our CSD-$\Delta\delta/\Delta T$ correlation method appear to display f_S values of 0.30−0.60 at the reference temperature used for calculating NH chemical shift deviations. The slope of the CSD-$\Delta\delta/\Delta T$ plot, in parts per thousand/°C, thus overestimates the actual rate of thermal loss of the structured state population by approximately a factor of 2.

The intercept of the correlation plot is given by the first two terms in eq 5. The first term corresponds to the population-weighted (at $T*$) average of the intrinsic thermal gradients of the structured and coil states and represents the limiting value of the intercept when thermal melting is minimal. Detailed simulations using eqs 1 and 3 with a wide range of reasonable values for the $(CSD)_S$ and Δgrad of the NHs, indicate that the intercept of an NH CSD-$\Delta\delta/\Delta T$ plot is given by eq 6, where

$$(\Delta\delta/\Delta T)_{CSD=0} = (\Delta\delta/\Delta T)_{rc} + f_S*[1 + 2m(T^m - T*)]\langle\Delta\text{grad}\rangle \quad (6)$$

T^m is the midpoint of the temperature range examined in the CSD-$\Delta\delta/\Delta T$ plot and $\langle\Delta\text{grad}\rangle$ is the average of Δgrad over all of the NHs included in the plot. So long as $T*$ is the lowest temperature used in the CSD/gradient plot, simulations for all reasonable values of $\langle\Delta\text{grad}\rangle$ indicate that large negative values of m will result in a gradient intercept approaching $(\Delta\delta/\Delta T)_{rc}$. For thermally stable structured states, the intercept approaches $(\Delta\delta/\Delta T)_{rc} + f_S*\langle\Delta\text{grad}\rangle$. All of the experimental data in Tables 1, 2, and 4 support this model; the observed intercepts are consistent with this prediction.

(61) Shalongo, W.; Dugad, L.; Stellwagen, E. *J. Am. Chem. Soc.* **1994**, *116*, 2500−2507.

Conclusions

We have introduced a novel graphic format for examining chemical shift data for amide NHs of proteins and peptides which correlates the temperature gradients with the chemical shift deviations from the reference coil values. In this format, slow-exchanging hydrogen-bonded sites in proteins can be determined with much higher confidence than using the value of the gradient alone. The method even appears to have some success in finding sites for which a partially populated hydrogen-bond state contributes without producing detectable exchange protection. An examination of Tables 1 and 2 shows that, independent of exchange rate classification, hydrogen-bonded NHs as a group display smaller negative $\Delta\delta/\Delta T$ values than those in the nonbonded category. However, for any individual NH observation, the prediction of H-bonded *versus* nonbonded status remains far from certain (prediction accuracies approach 80% for proteins).

The graph provides different but useful insights into systems that display conformational averaging: $\Delta\delta/\Delta T$ values should not be used to determine NH exposure in conformationally dynamic peptides. If the averaging is between a single structure which forms cooperatively and a random coil state, the plot is linear and displays a reasonable correlation coefficient ($R >$ 0.70). The slope of the plot is a measure of the increase in the mole fraction of the disordered coil state upon warming.

Our hypotheses concerning the relationship between the CSD/gradient correlation coefficient and cooperativity leads to several predictions concerning how this plot will respond to media- or mutation-associated changes in the extent to which the folded state of a peptide contributes to a conformational equilibrium. When only a very small population of the folded state is present in a sea of random coil conformers, the gradients will differ little from the random coil value and the range of NH-CSD values will also be limited. The loss in folded population upon warming is rather small and the slope of the correlation, if present, will be modest (−3 to −8 ppt/°C). If a single structure is enhanced by a medium change or residue mutation, as the folded state becomes more dominant in the conformational equilibrium (achieving mole fractions on the order of 0.35−0.7), the slope will increase and correlation coefficient should improve to >0.70. When the folded state population increases even further, the correlation coefficient should continue to improve but the slope will decrease unless the structure shows particularly facile and cooperative melting.

A comparison of the gradient/CSI plots (Figure 11) for [$Pen^{3,11}$,Nle^{7}]endothelin-1 in aqueous buffer with and without the addition of 15% HFIP provides an instructive example of the latter effect. This analogue appears to be the most structured endothelin analogue examined to date. Both CD spectroscopy and αH-CSD histograms recorded in the two media indicate that the helical domain is limited to Lys^9−Leu^{17} with Asp^8 as the N-cap and considerable C-terminal fraying in the absence of added HFIP.[22a] As expected on the basis of their location in the helix, the NHs for residues 12−15 display exchange half-lives in excess of 12 h at pH 3.4 (27 °C). Nonetheless, the NH of Pen^{15} displays a gradient of −10.9 ppb/°C in water. Upon addition of 15% HFIP, the NH of Pen^{15} moves 0.27 ppm downfield (suggesting a more persistent, stronger H-bond) and the gradient becomes less negative (−7.6 ppb/°C). Throughout the helical span, those NH temperature gradients that are outside of the $-1 \rightarrow -5.5$ ppb/°C range prior to HFIP addition become less extreme when HFIP is added. In Figure 11, this shows up as a decreased range of $\Delta\delta/\Delta T$ values and as a dramatic decrease in the slope of the gradient/CSD correlation for the helical residues with no change in correlation coefficient ($R = 0.92$).

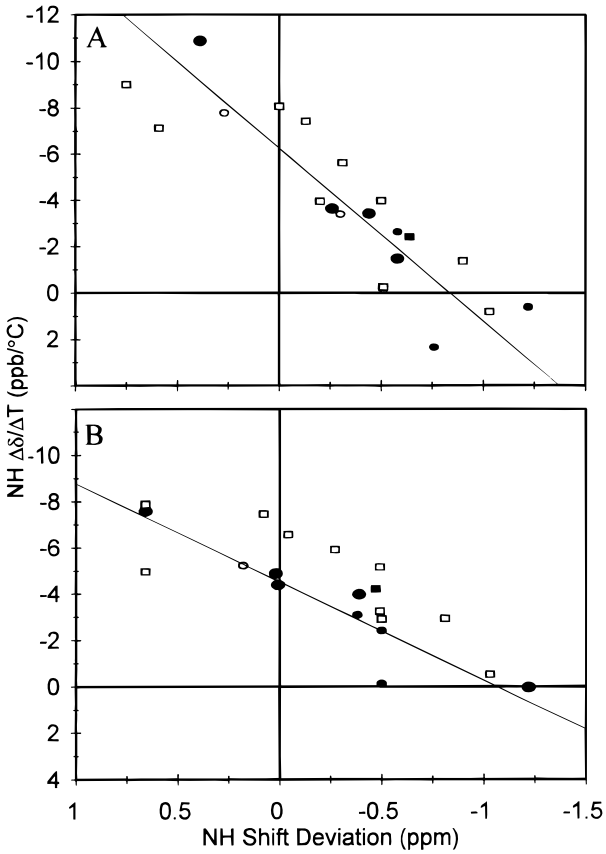

Figure 11. Amide NH CSD-$\Delta\delta/\Delta T$ plot for [Pen^{3,11},Nle^{7}]endothelin-1 at two levels of HFIP content in the medium (upper panel, no HFIP; lower panel, 15% HFIP). The least-squares line is derived from the NHs in the helical region, indicated by round symbols. The one exchange protected NH outside of the helical span is shown as a filled square. Open symbols indicate unprotected NHs. Those NHs which display in excess of a 20-fold exchange protection factor are shown as larger filled circles.

We attribute these changes to an increased stability of the helix upon addition of HFIP: there is less unfolding upon warming and, as a result, the $\Delta\delta/\Delta T$ values for the protected NHs approach those expected for the H-bonded state.

CSD-$\Delta\delta/\Delta T$ correlation plots should be useful in recognizing structuring in protein fragments. A secondary structure preference in a protein fragment which is proposed to have a "seeding" role in protein folding should represent a cooperative folding transition for a peptide which is limited to the sequence that folds. In our view, the use of NMR parameters (scalar and dipolar couplings) to derive the structural preference of a peptide sequence is justified only when the gradient/CSD plot displays a correlation coefficient greater than 0.70 and significant NH- and αH-CSD values (several |CSD| > 0.3). The instances in which a folded peptide state will dominate sufficiently but not melt on warming will be rare indeed and, thus, a small gradient will be a very poor predictor of H-bonding status for protein fragments. The partially populated H-bonded state should, in most cases, produce a downfield shift[62] for the H-bonded NHs. A decrease in folded state population on warming would, therefore, result in larger negative $\Delta\delta/\Delta T$ values rather than smaller ones. The slope of $\Delta\delta/\Delta T$ *versus* NH-CSD plots for structured peptides that randomize on warming generally are in the −8 to −20 ppt/°C range. Our model suggests that this reflects a *ca.* 0.04−0.10 decrease in the mole fraction of the folded state upon increasing the temperature 10 °C. The protein G B1 domain β-hairpin (residues 41−56) displays among the largest slopes observed, *ca.* −20 ppt/°C. Several additional examples of β-hairpin forming peptides which also display excellent CSD/gradient correlations have been published recently;[36] these and some others[35] appear in Table 4. There have been several instances[33e,36a] in which it has been suggested that peptides retain a significant secondary structure preference in the presence of ≥6 M urea; our analysis of the data for these systems confirms this suggestion. The observed $\Delta\delta/\Delta T$ values do not approach the value expected for the coil state and these systems retain a significant gradient/CSD correlation in aqueous urea.

The gradient/CSD correlation is also found for helical peptides. In the case of the C-peptide analogue examined herein, the degree of cooperativity displayed by such a short helix is, perhaps, surprising in light of current helix/coil transition models. Regarding this point, we note that long-range interactions—(a) Coulombic terms associated with Glu$^-$/His$^+$ and helix macrodipole, (b) medium- and long-range side chain/side chain interactions, 2-Glu$^-$/10-Arg$^+$ and 8-Phe/12-His—play a key role in the enhanced helix propensity.

We are currently attempting more quantitative correlations from NH shift temperature gradients and deviations, aiming to derive the free energy of folding and to distinguish between local and cooperative unfolding of designed helices. Our experience with additional peptides suggests three caveats regarding the gradient/CSD plot. (1) Aromatic sidechain conformational equilibria do not always yield trends toward the random coil value at neighboring residues upon warming. (2) Small peptides may display cold denaturation,[58a] an indication that hydrophobic forces are a particularly important driving force for the folding process. For the methods introduced in this paper to work, peptide structuring must increase upon cooling. We have observed positive slopes in NH CSD/gradient plots in instances of cold denaturation and for one other situation. (3) If a peptide is a predominantly disordered random coil at ambient temperatures, cooling may actual increase the relative contribution of the polyPro$_{II}$ conformation to the random coil equilibrium;[49] apparently this can lead to positive slopes. Our analyses to date indicate that when situation 3) applies, the gradients have smaller negative values than typical for a random coil. There have been instances[63] in which this observation, coupled an increase in $-[\theta]_{222}$ upon warming, led investigators to wrongly conclude that helical structuring increases with warming.

Returning to proteins, some residual correlation between chemical shift deviation and $\Delta\delta/\Delta T$ is observed for stable globular proteins that do not appear to be in equilibrium with a globally unfolded state. The observed slopes (−1.4 → −4.1 ppt/°C) are considerably smaller than those observed for peptides. Following the analysis we used for peptides, this suggests that the degree of structure randomization is considerably less in proteins. In most cases, the correlation is observed for unprotected or partially protected NHs. Some local structure randomization would be expected in protein loops and in helices with minimal tertiary structure contacts. However, the correlation has even been observed for the slowest exchanging NHs

(62) Those instances in which a presumably hydrogen-bonded NH appears upfield in partially formed turns, helices and in cyclic peptides can probably be rationalized as the result of weak intramolecular H-bonding in the folded state. In such cases, the folded state may sequester the NH from complete solvation thereby decreasing intermolecular H-bonding relative to the random coil state yielding an upfield shift.[12d] Due to unfolding upon warming, such NHs would display a less negative $\Delta\delta/\Delta T$ due to the increasing contribution of solvated species in the population weighted average at the higher temperature.

(63) For an example, see: Ilyina, E.; Milius, R; Mayo, K. H. *Biochemistry* **1994**, *33*, 13436−13444.

in β-sheets. This raises a number of questions. The protection factors for these NHs are very large, indicating that the contribution of locally nonbonded states cannot exceed 0.01 even at temperatures above ambient; significant backbone conformational changes cannot be proposed as the rationale for the remaining drift of NH shifts toward the random coil value upon warming. We suggest two alternative rationales: changes in side chain rotamer populations with temperature have quite pronounced effects on δ_{NH}, and/or increased backbone vibration decreases the size of the downfield shift associated with hydrogen bonding even though the NH remains fully sequestered from the solvent contact required for exchange. Careful measurement of the temperature dependence of $^{15}N-^{1}H$ relaxation data and ^{15}N shifts and an examination of the extent to which these correlate with the deviation of NH $\Delta\delta/\Delta T$ values from the expectation value for a hydrogen-bonded state should provide additional insights into both the sources of NH shift deviations and the nature of the residual dynamics observed in proteins. Such studies are in progress.

The model presented herein requires a significant positive ΔCp for the unfolding of peptides that display secondary structure preferences and linear δ_{NH} versus temperature plots. The latter features are commonly observed for peptide sequences that have been implicated as "folding determinants". If this model is correct, the formation of secondary structure prior to molten globule formation in a protein folding pathway would be consistent with the demonstrated importance of the hydrophobic effect in the earliest stages of protein folding. This provides new support for NMR studies of sequence fragment conformational preferences as a tool for understanding the earliest stages of protein folding. The NH gradient/shift-deviation plot should be useful in such studies.

Acknowledgment. The reported studies were partially supported by grants from the University of Washington Royalty Research Fund, Amylin Pharmaceuticals, and the Bristol-Myers Squibb Pharmaceutical Research Institute.

Supporting Information Available: Histograms of αH and NH shift deviations for the salmon calcitonin fragment (sCTf) in aqueous buffer and 25% HFIP and the temperature dependence of NH shift deviations for sCTf in 25% HFIP (2 pages). See any current masthead page for ordering and Internet access instructions.

JA963250H